RAMAN-ENHANCING, AND NON-LINEAR OPTICALLY ACTIVE NANO-SIZED OPTICAL LABELS AND USES THEREOF

ACKNOWLEDGMENT OF FEDERAL RESEARCH SUPPORT

[001] This invention was made, at least in part, with funding from the NIH (Award Numbers R01 GM068732 and P20 GM072021) and from the NSF (Award Number BES-0323453). Accordingly, the United States Government has certain rights in this invention.

BACKGROUND OF THE INVENTION

Field of the Invention

[002] The present invention relates to the creation of new classes of fluorescent, non-linear optically active and/or single molecule Raman active labels based on encapsulated noble metal nanoclusters, methods of preparing such labels, and methods of use thereof.

Background Art

[003] Single molecule fluorescence microscopy studies present an extreme limit in which weak signals must be observed on essentially zero background. Such optical methods relying on high-intensity laser excitation of highly emissive and robust fluorophores require extremely efficient background rejection. Relying on the introduction of artificial labels to identify the particular protein or structure of interest, fluorescence based methods suffer from two additional problems – photobleaching (loss of signal due to probe destruction) and autofluorescence (naturally occurring background fluorescence from native species within biological media). Even with these problems, fluorescence microscopy remains the primary optical method with potential for single molecule and chemical sensitivity while imaging biological media.

[004] Most *in vitro* fluorescent labeling is performed through standard chemical coupling of either N-succinimidyl ester-conjugated dyes to free, solvent-exposed amines (often on lysine residues) or maleimide-conjugated dyes to thiols on either naturally occurring or genetically introduced solvent-exposed cysteines. These

two coupling chemistries continue to be extremely useful in attaching small, highly fluorescent dyes to proteins of interest. Such fluorescent biomaterials are then adequate for *in vitro* single molecule studies, or they can be re-introduced into cells in high concentration either through microinjection or other membrane transport methods to perform bulk fluorescence studies of the protein of interest within whole cells. Not only can protein function be altered both by the size and point of attachment of the fluorescent label, but also often because of the coupling chemistry used, the site of the fluorescent labeling is not accurately known. Thus, the smallest possible genetically programmed label would be highly advantageous.

[005] Additionally, in biological systems, the autofluorescent background from flavins, porphyrins, and all other weakly fluorescent naturally occurring species can produce a large background that interferes with laser-induced fluorescence signals. Because of these problems, studying dynamics of few copies of proteins within living systems requires the development of new fluorescent probes that absorb and emit so strongly and without significant photobleaching such that they can be easily observed with extremely weak incoherent illumination for long times. Such illumination allows preferential excitation of the fluorophores of interest relative to that of weak background signals. Additionally, the weaker illumination would preserve biological viability by minimizing phototoxicity effects. Unfortunately, single molecule sensitivities are as of yet difficult to attain in such high background *in vivo* studies and are often difficult to observe even in lower background *in vitro* studies.

[006] Because of signal to noise constraints, single molecule studies are limited to fluorescence-based assays with all its associated difficulties. While single molecule methods have been effective in "peeling back" the ensemble average to examine environmental and mechanistic heterogeneity, current techniques require expensive laser-based equipment, specialized synthetic methods, and are still fundamentally limited by the poor optical properties or bioincompatibility of available fluorescent labels.

[007] Several key experiments have uniquely demonstrated the ability of single molecule microscopies to unravel the crucial steps leading to biological activity (Lu *et al.*, Science 1998, 282:1877-1882; Dickson *et al.*, Nature 1997, 388:355-358; Funatsu *et al.*, Nature 1995, 374:555-59; Ha *et al.*, Proc. Nat. Acad. Sci., USA 1996, 93, 6264-6268; Vale *et al.*, Nature 1996, 380:451-453; Deniz *et al.*, Proc. Natl. Acad. Sci., USA 2000, 97:5179-5184; Ha *et al.*, Proc. Natl. Acad. Sci. USA 1999, 96:893-

898; Harada *et al.*, Biophys. J. 1999, 76:709-715; Kinosita, Biophys. J. 2000, 78:149Wkshp). Most dramatic in studies of individual motor protein motion, mechanistic insights into protein function and substeps within biomechanical cycles can be directly visualized, without the need of difficult external synchronization (Funatsu *et al.*, Nature 1995, 374:555-59; Vale *et al.*, Nature 1996, 380:451-453; Kinosita, Biophys. J. 2000, 78:149Wkshp;Yanagida *et al.*, Curr. Opin. Cell Biol. 2000, 12:20-25). Even biomolecule folding has been probed to unravel pathways leading to both misfolded and folded states (Deniz *et al.*, Proc. Natl. Acad. Sci., USA 2000, 97:5179-5184; Ha *et al.*, Proc. Natl. Acad. Sci. USA 1999, 96:893-898). Now that orientational (Bartko, & Dickson, J. Phys. Chem. B 1999, 103:3053-3056; Bartko & Dickson, J. Phys. Chem. B 1999, 103:11237-11241; Bartko *et al.*, Chem. Phys. Lett. 2002, 358:459-465; Hollars & Dunn, J. Chem. Phys. 2000, 112:7822-7830) and fluorescence resonance energy transfer (FRET) methods (Weiss, Science 1999, 283:1676-1683) have been developed on the single molecule level, many more experiments are now possible. Unfortunately in all single molecule studies, researchers are relegated to artificial fluorescent labeling of proteins of interest and limited to *in vitro* observation. Re-introduction of labeled proteins into the cell has yet to produce viable *in vivo* single molecule signals due to the large autofluorescent background and poor photostability of organic fluorophores.

[008] Single molecules also have many inherently undesirable properties that limit the timescales of experiments. Excitation rates must be very high to yield biologically relevant information with reasonable time resolution (ms to seconds) and good signal to noise. Because the absorption cross-section (i.e. extinction coefficient, ε) of the best organic fluorophores is only ~10^{-16} cm^2 (i.e. $\varepsilon \sim 10^5$ M^{-1} cm^{-1}) at room temperature (Macklin *et al.*, Science 1996, 272:255-258), high intensity laser excitation must be utilized for single molecule fluorescence studies. Additionally, organic molecules can only withstand ~10^7 excitation cycles before they photochemically decompose (Dickson *et al.*, Nature 1997, 388:355-358; Lu & Xie, Nature 1997, 385:143-146; Macklin *et al.*, Science 1996, 272:255-258). At 10^6 excitations/second (using ~5kW/cm^2 excitation intensity and a typical collection/detection efficiency of 5%), this limits the time resolution to ~1 ms (with an idealized signal to noise ratio of ~7), and the average total time to follow an individual molecule before photobleaching of ~10 seconds. While this can be a very large amount of data on very biologically

relevant timescales, many of the excitation cycles end up being consumed by finding the molecules of interest before collecting data. Clearly, while reduction of oxygen can often increase the time before photobleaching, the photostability and overall brightness of the organic dyes limit all biological single molecule experiments. Thus, advances in fluorophore properties will be crucial to the continued success of all single molecule optical studies in biological systems.

[009] Requiring similar coupling chemistry to that of organic fluorophores, water soluble II-VI quantum dots have recently been proposed and demonstrated as biological labels (Bruchez *et al.*, Science 1998, 281:2013-2016; Chan & Nie, Science 1998, 281:2016-2018; Zhang *et al.*, Analyst 2000, 125:1029-1031). Materials such as CdSe with protective and stabilizing ZnS overcoatings have size dependent optical properties and can be synthesized with very narrow size distributions (Murray *et al.*, Z. Phys. D-Atoms Mol. Clusters 1993, 26:S231-S233; Murray *et al.*, J. Am. Chem. Soc. 1993, 115:8706-8715; Peng *et al.*, Nature 2000, 404:59-61). The strong absorption, spectral stability, and size-tunable narrow emission of these nanomaterials suggest exciting possibilities in biolabeling once further chemistry on the outer ZnS layer is performed to make these materials water-soluble (Rodriguez-Viejo *et al.*, J. Appl. Phys. 2000, 87:8526-8534; Dabbousi *et al.*, J. Phys. Chem. B 1997, 101:9463-9475). Because surface passivation is incredibly important in overall quantum dot optical properties, much care must be spent on quantum dot surface passivation and derivitization such that they can be reproducibly conjugated to proteins with predictable optical responses (Bruchez *et al.*, Science 1998, 281:2013-2016; Chan & Nie, Science 1998, 281:2016-2018; Rodriguez-Viejo *et al.*, J. Appl. Phys. 2000, 87:8526-8534; Dabbousi *et al.*, J. Phys. Chem. B 1997, 101:9463-9475; Nirmal & Brus, Acc. Chem. Res. 1999, 32:407-414; Nirmal *et al.*, Nature 1996, 383:802-804). In fact, successful implementation of water solubilization and surface passivation are only now beginning to bear fruit (Dubertret *et al.*, Science 2002, 298:1759-1762; Jaiswal *et al.*, Nat. Biotechnol. 2003, 21:47-51; Wu *et al.*, Nat. Biotechnol. 2003, 21:41-46; Sutherland, Curr. Opin. Solid State Mat. Sci. 2002, 6:365-370; Gao *et al.*, J. Biomed. Opt. 2002, 7:532-537; Mattoussi *et al.*, J. Am. Chem. Soc. 2000, 122:12142-12150).

[010] While quite promising due to their bright and very narrow size-dependent emission, multiple problems with using CdSe as biological labels still exist. Their synthesis requires high temperature methods using highly toxic precursors, they

are comparable to the size of proteins that they may label (2-6 nm in diameter), and they suffer from the same need to externally label proteins of interest and possibly re-introduce the labeled proteins into cells. Thus, while the strong oscillator strengths allow quantum dots to be easily observed with weak mercury lamp excitation, thereby avoiding much of the more weakly absorbing autofluorescent background, they are still not an ideal solution to *in vivo* or *in vitro* single molecule studies.

[011] In the 1970s, it was discovered that Raman (vibrational) signals are greatly enhanced (~106-fold) near roughened metal surfaces (Fleischmann *et al.*, J. Chem Soc. Comm, 1973 80-81; Fleischmann *et al.*, Chem Phys. Lett 1974, 26:163-166; Jeanmaire & van Duyne, J. Electroanal. Chem 1977, 84:1-20; Moskovits, M. *et al* J. Chem. Phys. 1978, 69: 4159-4161; King *et al.*, J. Chem Phys. 1978, 69:4472-4481). Originally postulated to arise from the strong electromagnetic field enhancements near silver surfaces, observed surface enhancements were often larger than could be ascribed to this effect alone. In 1984, Hildebrandt and Stockburger reported detection of ~10-9 M rhodamine 6G with SERS – a result requiring an enhancement of ~15 orders of magnitude (Hildebrandt, P. & Stockburger, M. *et al.*, J. Phys. Chem. 1984, 88: 5935-5944). This observation portended the recent reports of single molecule SERS (SM-SERS) that require a similar unexplainably large enhancement usually ascribed to nebulous electromagnetic and resonance Raman enhancements in the near field of silver nanoparticles (Kneipp *et al.*, Phys Rev. Lett. 1997, 78:1667-1670; Nie & Emory, Science 1997, 275:1102-1106; Michaels *et al.*, J. Am Chem Soc. 1999, 121:9932-9939; Weiss & Haran, Phys. Chem B 2001, 105: 12348-12354; Mooradian, *et al.*, Phys. Rev. Lett. 1969, 148: 873).

[012] SERS provides important vibrational information on molecules within complex chemical systems. Thus, while only certain modes are enhanced, surface enhanced Raman spectroscopy (SERS) is the only tool that can truly combine chemical information with single molecule sensitivity. Although Raman is a weak effect, it is actually stronger on the single molecule level than is fluorescence (Kneipp *et al.*, Phys Rev. Lett. 1997, 78: 1667-1670; Nie & Emory, Science 1997, 275: 1102-1106; Michaels *et al.*, J. Am Chem Soc. 1999, 121: 9932-9939; Hildebrandt & Stockburger, J. Phys. Chem. 1984, 88: 5935-5944). This results from the instantaneous nature of the Raman process, thereby increasing total emission rates and preventing photobleaching. Currently, SERS is impractical for labeling due to the need to amplify Raman signals with very large ($\geq$ 50-nm diameter) highly absorbing and scattering Au or Ag

nanoparticles as Raman contrast agents for molecules very close to the metallic surface (Fleischmann *et al.*, J. Chem Soc. Comm, 1973 80-81; Fleischmann *et al.*, Chem Phys. Lett 1974, 26:163-166; Jeanmaire & van Duyne, J. Electroanal. Chem 1977, 84: 1-20; Moskovits *et al.*, J. Chem. Phys. 1978, 69: 4159-4161; King *et al.*, J. Chem Phys. 1978, 69: 4472-4481; Hildebrandt & Stockburger, J. Phys. Chem. 1984, 88: 5935-5944; Moskovits *et al.*, Rev. Mod. Phys. 1985, 57: 783-824). As only a subset of particles give this enhanced response and the full enhancement cannot be explained with theory, the chemical and physical interactions giving rise to the enhancement and its associated fluorescent background remain elusive. Unfortunately, while Raman signals do not bleach, the large Ag and Au Raman contrast enhancing nanoparticles are incompatible with *in vivo* biological imaging.

[013] Due to its reliance on the presence of large nanoparticles for high Raman contrast, Raman imaging has yet to approach the single molecule level in anything even approximating a real biological system. Xie and co-workers have developed a novel zero-background non-linear optical microscopy, CARS, to image live cells with chemically relevant information (Cheng *et al.*, J. Phys. Chem. *B* 2001 105: 1277-1280; Cheng *et al.*, J. Phys. Chem. B 2002, 106: 8493-8498; Cheng *et al.*, Proc. Nat. Acad. Sci. USA 2003, 100: 9826-9830; Volkmer *et al.*, Appl. Phys. Lett. 2002, 80: 1505-1507; Cheng *et al.*, Biophys. J. 2002, 83: 502-509; Cheng *et al.*, J. Opt. Soc. Amer. B 2002, 19: 1363-1375). By probing the C-H stretch frequency, for example, they were able to differentiate lipids from cytoplasm and begin to image different organelle structures with good optical resolution and sensitivity. While promising, this exciting technique depends non-linearly on the number of vibrational modes of a given frequency in any molecule. Therefore, this method has yet to reach the sensitivity limits necessary to image and assay the dynamics of individual copies of a given protein. Clearly for linear and non-linear Raman imaging of living systems to reach the single molecule level, nanoscale Raman contrast agents must be created and specifically bound to proteins.

[014] Ideally, one would want the smallest possible genetically programmed label to be expressed on or adjacent to the protein of interest. Such an ideal label would need to have sufficiently strong absorption and emission as well as outstanding photostability to allow long time single molecule observation with high time resolution, even in the presence of high background fluorescence. Such a fluorescent probe does not yet exist. Currently the best available options due to being composed

solely of amino acids, green fluorescent protein (GFP; Dickson *et al.*, Nature 1997, 388:355-358; Heim, Proc. Nat. Acad. Sci., USA 1994, 91:12501-04; Ormo *et al.*, Science 1996, 273:1392-5; Chattoraj *et al.*, Proc. Nat. Acad. Sci., USA 1996, 93:362-67; Brejc *et al.*, Proc. Nat. Acad. Sci, USA 1997, 94:2306-11; Cubitt *et al.*, Trends in Biochem. Sci. 1995, 20:448-55; Kain & Kitts, Methods Mol. Biol. 1997, 63:305-24) and DsRed (Gross *et al.*, Proc. Natl. Acad. Sci., USA 2000, 97:11990-11995; Jakobs *et al.*, FEBS Lett. 2000, 479:131-135; Wall *et al.*, Nat. Struct. Biol. 2000, 7:1133-1138; Yarbrough *et al.*, Proc. Natl. Acad. Sci., USA 2001, 98:462-467) are excellent *in vivo* labels, and have been observed on the single molecule level in *in vitro* studies by many authors (Dickson *et al.*, Nature 1997, 388:355-358; Malvezzi-Campeggi *et al.*, Biophys. J. 2001, 81:1776-1785; Garcia-Parajo *et al.*, Proc. Natl. Acad. Sci., USA 2000, 97:7237-7242; Cotlet *et al.*, Chem. Phys. Lett. 2001, 336, 415-423; Lounis *et al.*, J. Phys. Chem. B 2001, 105:5048-5054; Garcia-Parajo *et al.*, Pure Appl. Chem. 2001, 73:431-434; Garcia-Parajo *et al.*, Chem. Phys. Chem. 2001, 2:347-360; Garcia-Parajo *et al.*, Proc. Natl. Acad. Sci., USA 2001, 98:14392-14397; Blum *et al.*, Chem. Phys. Lett. 2002, 362:355-361).

[015] In one of the first such studies, GFP's blinking and optical switching abilities have been studied as photons were used to shuttle the GFP chromophore between two different optically accessible states (Dickson *et al.*, Nature 1997, 388:355-358). Unfortunately, while GFP can be specifically attached to the N or C terminus of any protein and expressed *in vivo* as a highly fluorescent label, problems, especially on the single molecule level, still remain. GFP is 27kD or ~4 nm in diameter (Ormo *et al.*, Science 1996, 273:1392-5; Cubitt *et al.*, Trends in Biochem. Sci. 1995, 20:448-55), and can therefore be a large perturbation to the protein to which it is attached. In addition, emission only occurs once GFP has folded into its final conformation, a process that can take up to ~1 hour and, while examples of GFP labeling have been reported within all regions of different cells, sometimes GFP does not properly fold under a given set of conditions (Heim, Proc. Nat. Acad. Sci, USA 1994, 91:12501-04; Cubitt *et al.*, Trends in Biochem. Sci. 1995, 20:448-55). Additionally, when considering single molecule studies, its emission significantly overlaps with the autofluorescent background, but its emission intensity is only comparable to standard exogenous organic dyes, thereby making *in vivo* single molecule studies very challenging. While largely insensitive to oxygen, it also typically bleaches after ~10^7 excitation cycles, similar to standard organic dyes (Dickson *et al.*, Nature 1997, 388:355-358). DsRed

partially circumvents the issue of overlap with autofluorescent background, but while the red-shifted emission of DsRed relative to that of GFP could be an advantage, its comparable fluorescence intensity and tendency to form quadruplexes even at extremely low concentrations may further limit its use as an ideal biological label (Lounis *et al.*, J. Phys. Chem. B 2001, 105:5048-5054; Garcia-Parajo *et al.*, Chem. Phys. Chem. 2001, 2:347-360; Verkhusha *et al.*, J. Biol. Chem. 2001, 276:29621-29624; Sacchetti *et al.*, FEBS Lett. 2002, 525:13-19). Thus, the ideal label would combine the strong absorption, emission, and photostability of inorganic quantum dots, the small size and simple attachment chemistry of organic dyes, or preferably, like GFP and DsRed, the ability to be expressed *in vivo* as a single molecule biological label attached to any protein of interest without first purifying, labeling, and re-injecting the protein.

[016] In summary, while current labeling methods and materials have allowed myriad bulk studies and many *in vitro* single molecule experiments, single molecule experiments remain limited by the disadvantages of even the best fluorescent probes. There is a need in the art for new single molecule probes, created with greatly improved photostability, much stronger absorption and emission under weak illumination, facile synthesis and conjugation to proteins, and tunable emission color. Ideally, such fluorescent labels are genetically programmable such that proteins under study can be directly labeled intracellularly, without first being over-expressed, purified, labeled, and then reintroduced into cells.

SUMMARY OF THE INVENTION

[017] It is an object of the present invention to overcome, or at least alleviate, one or more of the difficulties or deficiencies associated with the prior art. The present invention fulfills in part the need to identify new, unique non-linear optically active labels, strongly fluorescent labels and/or Raman active labels that allow for the facile study of molecules at either single molecule or bulk concentrations. The compositions comprise a water-soluble label comprising an encapsulated noble metal nanocluster. In one embodiment, the noble metal nanocluster comprises between 2 and 8 noble metal atoms. In particular embodiments, the noble metal is selected from the group consisting of gold, silver, and copper. In certain embodiments, the noble metal nanocluster has a varying charge. In another embodiment, the nanocluster comprises 2- 31 metal atoms within the encapsulating scaffold.

[018] In one embodiment, the present invention encompasses a composition comprising a water-soluble label comprising a 2nd generation poly(amidoamine) dendrimer encapsulating a noble metal nanocluster, wherein the label has characteristic Raman bands, expressed in wavenumbers (cm^{-1}) as a shift in energy ranging from 100-3500 cm^{-1} from the excitation laser energy. In a second embodiment, it comprises a composition comprising a water-soluble label comprising a 4th generation poly(amidoamine) dendrimer encapsulating a noble metal nanocluster, wherein the label has characteristic Raman bands, expressed in wavenumbers (cm^{-1}) as a shift in energy ranging from 100-3500 cm^{-1} from the excitation laser energy. In a third embodiment, it comprises a composition comprising a water-soluble label comprising a peptide comprising a polypeptide sequence as defined in SEQ ID NO:1 encapsulating a noble metal nanocluster, wherein the label has characteristic Raman bands, expressed in wavenumbers (cm^{-1}) as a shift in energy ranging from 100-3500 cm^{-1} from the excitation laser energy.

[019] The invention is further directed to a composition comprising a water-soluble label comprising an encapsulated noble metal nanocluster, wherein the label has a single-molecule Raman spectrum. In one embodiment, the encapsulated noble metal nanocluster has a lifetime component of less than approximately 100 fs. In a further embodiment, the composition has a single molecule anti-Stokes spectrum. In another embodiment, the low excitation intensity is approximately 30 W/cm^2 at approximately 514 nm. In a further embodiment, the absorption cross section of the label is approximately $\sigma = 10^{-14}$ cm^2. In other embodiments, the Raman cross section of the label is approximately $\sigma = 10^{-14}$ cm^2.

[020] In certain other embodiments, the noble metal nanocluster is encapsulated in a peptide. Preferably the peptide is from approximately 5-500 amino acids in length. In other embodiments, the peptide is from approximately 5-20 amino acids in length. In one embodiment, the peptide comprises repeating amino acid dimers, preferably dimers of alanine and histidine. In a further embodiment, the peptide comprises a polypeptide sequence as defined in SEQ ID NO:1.

[021] In certain embodiments, the noble metal nanocluster is encapsulated in a dendrimer. In one embodiment, the dendrimer comprises poly(amidoamine), wherein the poly(amidoamine) dendrimer is selected from the group consisting of a 0th generation, 1st generation, 2nd generation, 3rd generation, a 4th generation, and a higher

generation poly(amidoamine) dendrimer. In another embodiment, the poly(amidoamine) dendrimer is a 2nd generation, or a 4th generation OH-terminated poly(amidoamine) dendrimer. The invention contemplates that the dendrimer may comprise a dendrimer core selected from the group consisting of:

(I) $H_2NCD_2CD_2NH_2$,

(II) 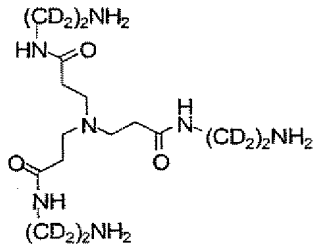

,

(III) 

,

(IV) 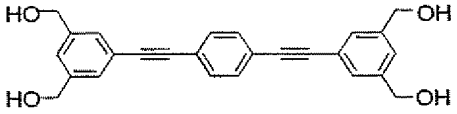

,

(V) 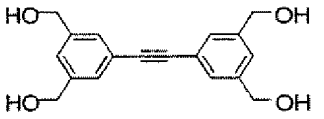

, and

(VI) 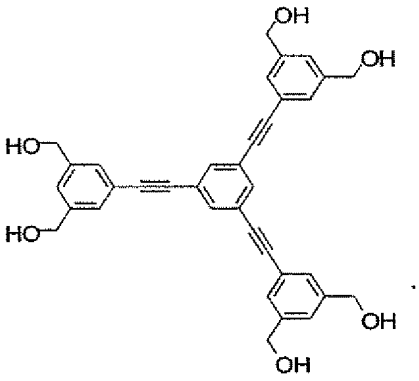

.

[022] The invention further contemplates that the encapsulated noble metal nanocluster further comprises a functional group having a single-molecule Raman spectrum. In one embodiment, the functional group is selected from the group consisting of C-D, C≡N, C≡C, and C≡O. In another embodiment, the functional group

has a vibrational frequency in the 1900~2300 cm^{-1} spectral region. The functional group may be located in any generation of a dendrimer.

[023] The invention encompasses a composition comprising a water-soluble label comprising an encapsulated noble metal nanocluster, wherein the label has a non-linear optical property. In one embodiment, the non-linear optical property is second harmonic generation. In one embodiment, the nanocluster is excited at approximately 860 nm, and an emission peak is observed at approximately 430 nm. In another embodiment, the encapsulated noble metal nanocluster has a lifetime component of less than approximately 100 ps, less than approximately 50 ps, less than approximately 25 ps, or less than approximately 10 ps. It is contemplated that the encapsulated noble metal nanocluster may have a two-photon-excited emission at 860 nm having a shorter excited state lifetime in comparison to that resulting from single photon excitation at 430-nm. It is also contemplated that the encapsulated noble metal nanocluster may have a two-photon-excited emission at 860 nm having the same excited state lifetime in comparison to that resulting from single photon excitation at 430 nm. In one embodiment, a two-photon fluorescence cross section of the label is greater than approximately 10^5 GM.

[024] The invention encompasses a composition comprising a water-soluble fluorescent label comprising an oligonucleotide encapsulated noble metal nanocluster. In certain embodiments, the oligonucleotide is from approximately 1-200 nucleotides in length. In other embodiments, the oligonucleotide is from 5-100, 10-50, 10-35, or approximately 12 nucleotides in length. In a further embodiment, the oligonucleotide comprises a nucleotide sequence as defined in SEQ ID NO:2, or is a polyA, polyG, polyT, or polyC sequence, including C_{12} (SEQ ID NO:3), C_{24} (SEQ ID NO:4), C_{36} (SEQ ID NO:5), T_{12} (SEQ ID NO:6), A_{12} (SEQ ID NO:7), and G_{12} (SEQ ID NO:8). In one embodiment, one noble metal nanocluster binds to the oligonucleotide, and the encapsulated nanocluster comprises 4 or fewer noble metal atoms.

[025] The invention contemplates a method of preparing an oligonucleotide encapsulated noble metal nanocluster capable of fluorescing, comprising the steps of: (a) combining an oligonucleotide, an aqueous solution comprising a noble metal, and distilled water to create a combined solution; (b) adding a reducing agent; (c) subsequently adding a sufficient amount of an acidic compound to adjust the combined solution to a neutral range pH; and (d) mixing the pH adjusted, combined solution to allow the formation of the oligonucleotide encapsulated noble metal nanocluster. In

one embodiment, the reducing agent is selected from the group consisting of light, a chemical reducing agent, a photochemical reducing agent and a combination thereof. It is contemplated that the noble metal to oligonucleotide molar ratio in step a) is approximately 0.1:1. In one embodiment, the label exhibits a polarized spectral emission and exhibits a dipole emission pattern.

[026] Preferably, the label has a spectral emission that provides information about the label's environment and/or biological state, wherein the biological state is selected from the group consisting of a quantitative and qualitative presence of a biological moiety; structure, composition, and conformation of a biological moiety; localization of a biological moiety in an environment; an interaction between biological moieties, an alteration in structure of a biological compound, and an alteration in a cellular process.

[027] Preferably the fluorescent label of the present invention is capable of fluorescing over a pH range of approximately 3 to approximately 10, and the noble metal nanocluster emits greater than approximately 10^6 photons, greater than 10^7, greater than 10^8, or greater than 10^9 photons before photobleaching. In one embodiment, the encapsulated noble metal nanocluster has a fluorescence quantum yield of greater than approximately 1% and a saturation intensity ranging from approximately 1 to 10^6 W/cm^2 at a nanocluster spectral excitation maximum. In certain embodiments, the low excitation intensity is approximately 30 W/cm^2 at approximately 460 nm.

[028] The present invention further encompasses methods of using the labels described herein in order to study a biological state. The invention provides for a method of monitoring a molecule of interest comprising: a) attaching a water-soluble label comprising an encapsulated noble metal nanocluster to a molecule of interest, wherein the label emits an emission spectrum over a certain range of visible or near infrared wavelengths; and b) detecting the emission or emission spectrum of the label. In certain embodiments, the method further comprises the initial step of attaching a linker molecule to the encapsulated noble metal nanocluster, wherein the linker molecule is capable of attaching the label to the molecule of interest. In one embodiment, the molecule of interest is present in a biological sample.

BRIEF DESCRIPTION OF THE DRAWINGS

[029] Figure 1A provides UV-Visible absorption spectra of aqueous silver/dendrimer solutions. (1) indicates strong plasmon absorption (398 nm) characteristic of large, non-fluorescent dendrimer-encapsulated silver nanoparticles prepared through $NaBH_4$ reduction of silver ions in the dendrimer host (1:12 dendrimer:Ag). (2) indicates the absorption spectrum of unreduced, non-fluorescent 1:3 (dendrimer:Ag) solution before photoactivation, and (3) indicates the same solution after photoactivation/photoreduction to produce highly fluorescent silver nanodots. Figure 1B provides electrospray ionization mass spectrum of photoactivated G2-OH PAMAM (MW: 3272 amu) – $AgNO_3$ solution. Ag_n nanodot peaks are spaced by the Ag atomic mass (107.8 amu) and only appear in the fluorescent, photoactivated nanodot solutions.

[030] Figures 2A-D show mercury lamp excited (450 to 480 nm, 30W/cm^2, scale bar = 15 μm) epifluorescence microscopy images demonstrating time-dependent photoactivation of aqueous dendrimer-encapsulated silver nanodots. Each 300 ms CCD frame shows increasing fluorescence with illumination time at 0 seconds, 0.3 seconds, 1.5 seconds, and 6 seconds. Figure 2E shows surface-bound silver nanodot emission patterns in aqueous solutions. Indicative of single molecules, the anisotropic emission patterns and fluorescence blinking are easily observable under weak Hg lamp excitation.

[031] Figure 3 shows room temperature single nanodot confocal fluorescence spectra (476-nm Ar^+ laser excitation, 496-nm long-pass filter, dispersed by a 300-mm monochromator). Emission maxima for the five typical nanodots shown are 533 nm, 553 nm, 589 nm, 611 nm, and 648 nm. The ensemble fluorescence spectrum of bulk silver nanodot solutions (top) largely consists of these five spectral types, which are indistinguishable from that on AgO surfaces.

[032] Figures 4A shows a single nanodot fluorescence lifetime and 5B shows saturation intensity measurements of typical dendrimer-encapsulated nanodots. In 5A, 400-nm excited lifetimes are limited by the 300 ps instrument response, but indicate a sub-100 ps component (92%) and a 1.6 ns component (8%) after deconvolution. In 4B, saturation occurs at ~400 W/cm^2 (using off resonant, 514.5-nm excitation), with total intensity differences arising from variations in quantum yields among various nanodots. The organic dye, $DiIC_{18}$, for comparison, has a saturation intensity of

10kW/cm^2. Comparisons to DiI yield a lower estimate of the fluorescence quantum yield of ~30%.

[033] Figure 5A shows UV-Vis absorption spectra of aqueous gold nanodot and pure dendrimer solutions. Figure 5B shows subtraction of absorption spectra in A revealing the 384-nm absorption of PAMAM encapsulated Au nanodots.

[034] Figure 6 shows excitation and emission spectra of G4-OH PAMAM encapsulated gold nanoclusters at room temperature. The excitation spectrum is denoted by "1", while the emission spectrum is denoted with "2."

[035] Figure 7A shows lifetime measurement of gold nanodots in aqueous solution. Instrumental response and nanodot data with fit exhibit the 7.5 ns (93%) and 2.8 μs (7%) lifetimes. Figure 7B shows ESI mass spectrum of G2-OH PAMAM encapsulated gold nanodots with expected m/z of 4940 for G2-OH + Au_8 +$5H_2O$ + H^+.

[036] Figure 8 shows the excitation and emission spectra of PAMAM dendrimer encapsulated copper nanoclusters at room temperature. The excitation spectrum is denoted by "1", while the emission spectrum is denoted with "2."

[037] Figure 9 shows the response of the electronic transition of the oligonucleotide bases to association with Ag^+ and Ag nanoclusters. Following are the conditions for the spectra: A (dotted line) - 10 μM oligonucleotide solution; B (solid line) – oligonucleotide with 60 μM Ag^+ (1 Ag^+:2 bases); C (coarse dashed line) – 2 min. after adding 1 BH_4^-:1 Ag^+ to the oligonucleotide/Ag^+ solution; D (fine dashed line) - 1100 min after adding BH_4^- to the oligonucleotide/Ag^+ solution.

[038] Figure 10 shows the response of the circular dichroism associated with electronic transition of the oligonucleotide bases to association with Ag^+ and Ag nanoclusters. Following are the conditions for the spectra: A (dotted line) - 10 μM oligonucleotide solution; B (solid line) – oligonucleotide with 60 μM Ag^+ (1 Ag^+:2 bases); C (coarse dashed line) – 120 min. after adding 1 BH_4^-:1 Ag^+ to the oligonucleotide/Ag^+ solution; D (fine dashed line) - 4300 min after adding BH_4^- to the oligonucleotide/Ag^+ solution.

[039] Figures 11A-D show electrospray ionization mass spectra. Figure 3A shows the electrospray ionization mass spectra of the oligonucleotide and silver ion adducts. Following are the conditions for the spectra: Left axis - 75 μM oligonucleotide solution with a peak at 3607 amu; Right axis – 75 μM oligonucleotide with 60 μM Ag^+ (1 Ag^+:2 bases) with peaks at 3821, 3928, 4035, 4141, and 4247 amu.

The intensities of the peaks for the Ag^+/DNA complexes were fit with a Poisson distribution (open circles) to give a mean size of 4.3 ± 1.3 Ag^+/oligonucleotide. Figures 11B-D show electrospray ionization mass spectra of silver cluster complexes with the DNA oligonucleotide. Overlaid as open circles are the Poisson fits of the intensity distributions and the mean number of bound Ag is provided in the parentheses. Following are the conditions for the spectra: (B) 75 μM oligonucleotide with 60 μM Ag^+ and 50 minutes after adding 1 BH_4^-:1 Ag^+ (1.8 ± 0.3 Ag); (C) 350 minutes after adding BH_4^- to the oligonucleotide/Ag^+ solution (2.4 ± 0.2 Ag); (D) 1050 minutes after adding BH_4^- to the oligonucleotide/Ag^+ solution (3.0 ± 0.2 Ag). The peaks are observed at 3607, 3714, 3821, 3927, and 4036 amu. The small peaks displaced by 22 amu are attributed to Na-DNA adducts due to the use of $NaBH_4^-$ for the reduction.

[040] Figure 12 shows absorption spectra associated with the DNA-bound silver nanoclusters . For these spectra, [oligonucleotide] = 10 μM, [Ag^+] = 60 μM, and [BH_4^-] = 60 μM. The foremost spectrum in the time series was acquired 9 minutes after adding the BH_4^-, and it has λ_{max} = 426 nm. Subsequent spectra were acquired approximately every 30 minutes. The inset spectrum shows the last spectrum in the series (692 minutes) and peaks are observed at 424 and 520 nm.

[041] Figure 13 shows induced circular dichroism spectra for the electronic transitions associated with the nanoclusters. For these spectra, [oligonucleotide] = 10 μM, [Ag^+] = 60 μM, and [BH_4^-] = 60 μM in a 1 mM phosphate buffer and the cell path-length was 5 cm. The spectra were collected 2 min (A – dashed-dotted line), 20 min (B – dotted line), 40 min (C – fine dashed line), 60 min (D – coarse dotted line), and 150 minutes (E – solid line) after adding the BH_4^-.

[042] Figures 14A-B show fluorescence emission spectrum of the silver nanoclusters bound to the oligonucleotide. For these spectra, [oligonucleotide] = 10 μM, [Ag^+] = 60 μM, and [BH_4^-] = 60 μM. In (A), a series of emission spectra were acquired using 240, 260, 280, and 300 nm excitation. A broad emission band is observed between 400 and 550 nm and a peak is observed at 632 nm. In (B), excitation at 540, 560, and 580 nm results in emission bands with maxima at 629, 638, and 642 nm, respectively.

[043] Figure 15 shows the aromatic proton region from ^1H NMR spectra of the oligonucleotide with and without the silver nanoclusters. Vertical lines indicate

aromatic proton resonances with chemical shifts that change after nanocluster formation. Cytosine H6 resonances, which exhibit the largest changes in chemical shift, can be identified by their splitting due to coupling to cytosine H5. For these spectra, [oligonucleotide] = 0.93 mM, $[Ag^+]$ = 5.6 mM, and $[BH_4^-]$ = 5.6 mM in a solution of 90% 1 mM phosphate buffer and 10% D_2O at 25°C.

[044] Figure 16A-B show the absorption spectra associated with the DNA-bound silver nanoclusters using 1 Ag^+:10 bases. For these spectra shown at (A), [oligonucleotide] = 10 μM, $[Ag^+]$ = 12 μM, and $[BH_4^-]$ = 12 μM. The first ten spectra were acquired every 2 minutes after adding the BH_4^-, and the spectrum at 20 minutes has λ_{max} = 440 and 357 nm. Subsequent spectra were acquired approximately every 40 minutes. The inset spectrum (B) shows the last spectrum in the series (704 minutes) and a peak at 380 nm is observed. In addition, a broad emission band from 430 – 600 nm is observed.

[045] Figure 17A-F show (A) Dark-field and (B) Stokes-shifted emission images from individual peptide-encapsulated 2-8 atom Ag nanoclusters within the same field of view. (C) Emission spectrum of a single peptide encapsulated Ag_n nanocluster positioned between the monochromator slits (vertical white lines) excited at 514.5 nm, 30W/cm^2. (D) PAMAM-encapsulated Ag_n dark-field and (E) Stokes-shifted emission image of the same field of view. (F) Emission spectrum of a dendrimer encapsulated Ag nanocluster. Dark field scattering arises only from glass imperfections and is completely uncorrelated with emissive features.

[046] Figure 18A shows summed Raman spectra from 100 PAMAM- (o) and 100 peptide-encapsulated (*) Ag_n nanoclusters. Spectral subtractions remove the similar nanocluster fluorescent background and yield characteristic (B) dendrimer and (C) peptide Raman lines when only positive peaks are retained for each subtraction order.

[047] Figure 19 shows blinking of Raman emission from PAMAM encapsulated Ag nanodot indicating single molecule Raman signals arising from the nanocluster-scaffold interaction.

[048] Figure 20A shows Stokes- (right, positive shifts to lower energy) and anti-Stokes- (left, negative shifts to higher energy) shifted Raman spectra for an individual dendrimer-encapsulated Ag nanocluster. AS-shifted frequencies match exactly with their Stokes counterparts. Lower (gray) Stokes-shifted spectrum shows

fluorescence observed from the dendrimer encapsulated nanocluster when Raman scattering has blinked off. (B) With the same spectral axis as (A), three successive 10-second frames show intermittency of the AS emission. C is the expanded AS spectrum from A.

[049] Figure 21 shows six proposed dendrimer cores.

[050] Figure 22A-E show multifunctionalization strategies for dendrimers. A shows a single functionalized dendrimer, B shows a combination of different functionalized dendrons, C shows random difunctionalization, D shows the use of multifunctionalized monomers, and E shows a combination of the strategies shown in B and D.

[051] Figure 23 shows the emission spectrum from two-photon excitation of bulk dendrimer encapsulated silver nanodots (top, bold spectrum) compared to single-molecule emission from one photon excitation. The second harmonic generation is indicated by *; its peak appears at double the frequency (430 nm) of excitation with the same spectral width. Fluorescence is shown by the broader peak.

[052] Figure 24 shows two-photon excited emission power dependence, demonstrating that emission intensity is quadratic with respect to incident intensity. Total fluorescence emission was measured against laser power for bulk dendrimer encapsulated silver nanodots.

[053] Figure 25 shows the two-photon excited emission radiative lifetime, demonstrating that the decay time of the bulk dendrimer encapsulated silver nanodots is limited by the instrument response function. The instrument response function was measured with frequency doubled Ti-sapphire 860 nm argon-pumped laser.

DETAILED DESCRIPTION OF THE INVENTION

[054] The present invention provides compositions comprising a non-linear optically active, fluorescent and/or Raman active label, methods for preparing the compositions and methods of using the compositions. The compositions of the present invention comprise encapsulated noble metal nanoclusters that, in one embodiment, are capable of fluorescing. In further embodiments, the compositions of the present invention comprise encapsulated noble metal nanoclusters having single molecule Raman spectra specific to the encapsulating material. In other embodiments, the

compositions of the present invention exhibit frequency doubling and/or multiphoton excited fluorescence.

[055] Unless otherwise noted, the terms used herein are to be understood according to conventional usage by those of ordinary skill in the relevant art. In addition to the definitions of terms provided below, definitions of common terms in molecular biology may also be found in Rieger *et al.*, 1991 Glossary of genetics: classical and molecular, 5th Ed., Berlin: Springer-Verlag; and in Current Protocols in Molecular Biology, F.M. Ausubel *et al.*, Eds., Current Protocols, a joint venture between Greene Publishing Associates, Inc. and John Wiley & Sons, Inc., (1998 Supplement). It is to be understood that as used in the specification and in the claims, "a" or "an" can mean one or more, depending upon the context in which it is used. Thus, for example, reference to "a cell" can mean that at least one cell can be utilized.

[056] The present invention may be understood more readily by reference to the following detailed description of the preferred embodiments of the invention and the Examples included herein. However, before the present compounds, compositions, and methods are disclosed and described, it is to be understood that this invention is not limited to specific noble metals, specific encapsulating materials, specific functional groups, specific polypeptides, specific oligonucleotides, specific dendrimers, specific conditions, or specific methods, etc., as such may, of course, vary, and the numerous modifications and variations therein will be apparent to those skilled in the art. It is also to be understood that the terminology used herein is for the purpose of describing specific embodiments only and is not intended to be limiting.

[057] In one embodiment, the present invention encompasses a composition comprising a water-soluble label comprising a 2^{nd} generation poly(amidoamine) dendrimer encapsulating a noble metal nanocluster, wherein the label has characteristic Raman bands, expressed in wavenumbers (cm^{-1}) as a shift in energy ranging from 100-3500 cm^{-1} from the excitation laser energy. In a second embodiment, it comprises a composition comprising a water-soluble label comprising a 4^{th} generation poly(amidoamine) dendrimer encapsulating a noble metal nanocluster, wherein the label has characteristic Raman bands, expressed in wavenumbers (cm^{-1}) as a shift in energy ranging from 100-3500 cm^{-1} from the excitation laser energy. In a third embodiment, it comprises a composition comprising a water-soluble label comprising a peptide comprising a polypeptide sequence as defined in SEQ ID NO:1 encapsulating a noble metal nanocluster, wherein the label has characteristic Raman bands, expressed

in wavenumbers (cm^{-1}) as a shift in energy ranging from 100-3500 cm^{-1} from the excitation laser energy.

[058] The invention is further directed to a composition comprising a water-soluble label comprising an encapsulated noble metal nanocluster, wherein the label has a single-molecule Raman spectrum. In one embodiment, the encapsulated noble metal nanocluster has a lifetime component of less than approximately 100 fs. In a further embodiment, the composition has a single molecule anti-Stokes spectrum. In another embodiment, the low excitation intensity is approximately 30 W/cm^2 at approximately 514 nm. In a further embodiment, the absorption cross section of the label is approximately $\sigma = 10^{-14}$ cm^2. In other embodiments, the Raman cross section of the label is approximately $\sigma = 10^{-14}$ cm^2.

[059] In certain other embodiments, the noble metal nanocluster is encapsulated in a peptide. Preferably the peptide is from approximately 5-500 amino acids in length. In other embodiments, the peptide is from approximately 5-20 amino acids in length. In one embodiment, the peptide comprises repeating amino acid dimers, preferably dimers of alanine and histidine. In a further embodiment, the peptide comprises a polypeptide sequence as defined in SEQ ID NO:1.

[060] In certain embodiments, the noble metal nanocluster is encapsulated in a dendrimer. In one embodiment, the dendrimer comprises poly(amidoamine), wherein the poly(amidoamine) dendrimer is selected from the group consisting of a 0^{th} generation, 1^{st} generation, 2^{nd} generation, 3^{rd} generation, a 4^{th} generation, and a higher generation poly(amidoamine) dendrimer. In another embodiment, the poly(amidoamine) dendrimer is a 2^{nd} generation, or a 4^{th} generation OH-terminated poly(amidoamine) dendrimer. The invention contemplates that the dendrimer may comprise a dendrimer core selected from the group consisting of:

(I) $H_2NCD_2CD_2NH_2$,

(II) 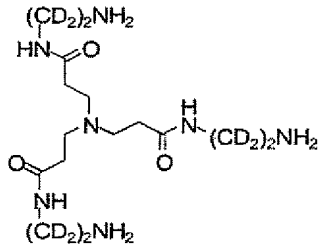

,

(III)  ,

(IV) 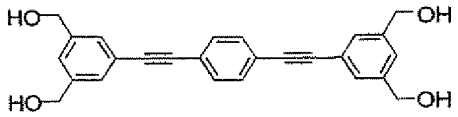 ,

(V) 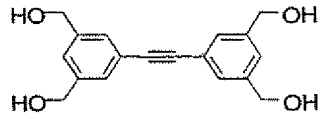 , and

(VI) 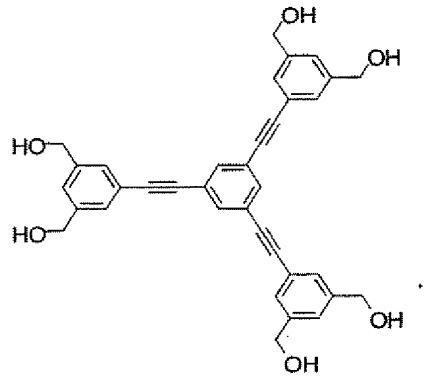 .

[061] The invention further contemplates that the encapsulated noble metal nanocluster further comprises a functional group having a single-molecule Raman spectrum. In one embodiment, the functional group is selected from the group consisting of C-D, C≡N, C≡C, and C≡O. In another embodiment, the functional group has a vibrational frequency in the 1900~2300 cm^{-1} spectral region. The functional group may be located in any generation of a dendrimer.

[062] The invention encompasses a composition comprising a water-soluble label comprising an encapsulated noble metal nanocluster, wherein the label has a non-linear optical property. In one embodiment, the non-linear optical property is second harmonic generation. In one embodiment, the nanocluster is excited at approximately 860 nm, and an emission peak is observed at approximately 430 nm. In another embodiment, the encapsulated noble metal nanocluster has a lifetime component of less than approximately 100 ps, less than approximately 50 ps, less than approximately 25 ps, or less than approximately 10 ps. It is contemplated that the encapsulated noble metal nanocluster may have a two-photon-excited emission at 860 nm having a shorter excited state lifetime in comparison to that resulting from single photon excitation at

430-nm. It is also contemplated that the encapsulated noble metal nanocluster may have a two-photon-excited emission at 860 nm having the same excited state lifetime in comparison to that resulting from single photon excitation at 430 nm. In one embodiment, a two-photon fluorescence cross section of the label is greater than approximately 10^5 GM.

[063] The invention encompasses a composition comprising a water-soluble fluorescent label comprising an oligonucleotide encapsulated noble metal nanocluster. In certain embodiments, the oligonucleotide is from approximately 1-200 nucleotides in length. In other embodiments, the oligonucleotide is from 5-100, 10-50, 10-35, or approximately 12 nucleotides in length. In a further embodiment, the oligonucleotide comprises a nucleotide sequence as defined in SEQ ID NO:2, or is a polyA, polyG, polyT, or polyC sequence, including CCCCCCCCCCCC (SEQ ID NO:3), CCCCCCCCCCCCCCCCCCCCCCCC (SEQ ID NO:4), CCCCCCCCCCCCCCCCCCCCCCCCCCCCCCCCCCCC (SEQ ID NO:5), TTTTTTTTTTTT (SEQ ID NO:6), AAAAAAAAAAAA (SEQ ID NO:7), and GGGGGGGGGGGG (SEQ ID NO:8). In one embodiment, one noble metal nanocluster binds to the oligonucleotide, and the encapsulated nanocluster comprises 4 or fewer noble metal atoms.

[064] The invention contemplates a method of preparing an oligonucleotide encapsulated noble metal nanocluster capable of fluorescing, comprising the steps of: (a) combining an oligonucleotide, an aqueous solution comprising a noble metal, and distilled water to create a combined solution; (b) adding a reducing agent; (c) subsequently adding a sufficient amount of an acidic compound to adjust the combined solution to a neutral range pH; and (d) mixing the pH adjusted, combined solution to allow the formation of the oligonucleotide encapsulated noble metal nanocluster. In one embodiment, the reducing agent is selected from the group consisting of light, a chemical reducing agent, a photochemical reducing agent and a combination thereof. It is contemplated that the noble metal to oligonucleotide molar ratio in step a) is approximately 0.1:1. In one embodiment, the oligonucleotide encapsulated noble metal nanocluster is capable of fluorescing. In one embodiment, the label exhibits a polarized spectral emission and exhibits a dipole emission pattern.

[065] Preferably the fluorescent label of the present invention is capable of fluorescing over a pH range of approximately 3 to approximately 10, and the noble metal nanocluster emits greater than approximately 10^6 photons, greater than 10^7,

greater than 10^8, or greater than 10^9 photons before photobleaching. In one embodiment, the encapsulated noble metal nanocluster has a fluorescence quantum yield of greater than approximately 1% and a saturation intensity ranging from approximately 1 to 10^6 W/cm^2 at a nanocluster spectral excitation maximum. In certain embodiments, the low excitation intensity is approximately 30 W/cm^2 at approximately 460 nm.

[066] The present invention further encompasses methods of using the labels described herein in order to study a biological state. The invention provides for a method of monitoring a molecule of interest comprising: a) attaching a water-soluble label comprising an encapsulated noble metal nanocluster to a molecule of interest, wherein the label emits an emission spectrum over a certain range of visible or near infrared wavelengths; and b) detecting the emission or emission spectrum of the label. In certain embodiments, the method further comprises the initial step of attaching a linker molecule to the encapsulated noble metal nanocluster, wherein the linker molecule is capable of attaching the label to the molecule of interest. In one embodiment, the molecule of interest is present in a biological sample.

[067] The present invention provides for compositions comprising a water-soluble label comprising an encapsulated noble metal nanocluster. In one embodiment, the noble metal nanocluster comprises between 2 and 8 noble metal atoms. In preferred embodiments, the noble metal is selected from the group consisting of gold, silver, and copper. In another embodiment, the nanocluster comprises between 2 and 31 noble metal atoms.

[068] In one embodiment, the label is a fluorescent label that exhibits a polarized spectral emission and/or a dipole emission pattern. In a further embodiment, the fluorescent label of the present invention is capable of fluorescing over a pH range of approximately 3 to approximately 10, and the noble metal nanocluster emits greater than approximately 10^6 photons before photobleaching. In a further embodiment, the noble metal nanocluster emits greater than approximately 10^7, 10^8, 10^9, 10^{10} or greater than 10^{11} photons before photobleaching. In one embodiment, the encapsulated noble metal nanocluster has a fluorescence quantum yield of greater than approximately 1% and a saturation intensity ranging from approximately 1 to 10^6 W/cm^2 at a nanocluster spectral excitation maximum. In certain embodiments, the low excitation intensity is approximately 30 W/cm^2 at approximately 460 nm.

[069] The present invention further encompasses methods of using the labels in order to study a biological state. Preferably the label has a spectral emission that provides information about a biological state, wherein the biological state is selected from the group consisting of a quantitative and qualitative presence of a biological moiety; location, structure, composition, and conformation of a biological moiety; localization of a biological moiety in an environment; an interaction between biological moieties, an alteration in structure of a biological compound, and an alteration in a cellular process. The invention provides for a method of monitoring a molecule of interest comprising: a) attaching a label comprising an encapsulated noble metal nanocluster to a molecule of interest, wherein the label emits an emission spectrum over a certain range of visible and near infrared wavelengths; and b) detecting the emission or emission spectrum of the label. In certain embodiments, the label further comprises a functional group having a single molecule Raman spectra. In certain embodiments, the method further comprises the initial step of attaching a linker molecule to the encapsulated noble metal nanocluster, wherein the linker molecule is capable of attaching the label to the molecule of interest. In a preferred embodiment, the molecule of interest is present in a biological sample. In one preferred embodiment, the noble metal nanocluster is encapsulated in a peptide. In one embodiment, the peptide is expressed in a cell. In one embodiment, the peptide comprises a fusion polypeptide.

[070] The water-soluble noble metal nanoclusters (nanodots) described herein are easily observed as single nanodots with weak mercury lamp excitation due to their incredibly strong absorption and emission (Peyser *et al.*, Science 2001, 291:103; Peyser *et al.*, J. Phys. Chem. B 2002, 106:7725). With absorption strengths comparable to those of much larger quantum dots, these highly fluorescent and incredibly photostable nanodots are useful, in one embodiment, as single molecule and bulk fluorescent biolabels. The creation of stable, biocompatible individual noble metal nanoclusters greatly facilitates the use of these photoactivated nanomaterials as extremely small, bright fluorophores. Such bright, easily synthesized, robust nanomaterials of the present invention will expand the accessibility of single molecule methods by greatly decreasing experimental cost and complexity and providing optically excited fluorophores capable of producing orders of magnitude more photons from individual molecules than currently possible. Furthermore, the nanodots described herein are easily observed as having single molecule Raman spectra that are

specific to the encapsulating material, and/or to any functional groups contained therein. In addition, the nanodots described herein may demonstrate non-linear

[071] One aspect of the invention described herein provides the production and characterization of extremely robust, incredibly bright, photoactivated biological labels that are simultaneously very small, biocompatible, suitable for specific *in vitro* and *in vivo* labeling and easily observed on the single molecule level with only weak mercury lamp excitation. Typically at least 20 times brighter than the best organic dyes, the brightness and ease of synthesis allows researchers to easily perform single molecule experiments with standard, inexpensive, lamp-based fluorescence microscopes. As described herein, only a few atoms to few tens of atoms of a noble metal are necessary to generate extremely bright compounds easily observed on the single molecule level. As a result, the proper biocompatible scaffold (generally a dendrimer, genetically optimized peptide, or any other appropriate encapsulating material) encapsulating the noble metal nanoclusters makes these very useful and potentially the smallest possible *in vivo* and *in vitro* labels.

[072] As used herein, "encapsulating material" refers to a substrate that is capable of attaching to, or physically associating with one or molecules of a noble metal nanocluster. An encapsulating material can provide a means for attaching the noble metal nanocluster indirectly to a molecule of interest, and can protect the noble metal nanocluster from the environment. The attachment or linkage is by means of covalent bonding, hydrogen bonding, adsorption, metallic bonding, van der Waals forces or ionic bonding, or any combination thereof. As used herein, "encapsulated" means that one or more molecules of the noble metal nanocluster can be physically associated with or entrapped within the encapsulating material, dispersed partially or fully throughout the encapsulating material, or attached or linked to the encapsulating material or any combination thereof, whereby the attachment or linkage is by means of covalent bonding, hydrogen bonding, adsorption, metallic bonding, van der Waals forces or ionic bonding, or any combination thereof.

[073] The noble metal nanoclusters encompassed by the present invention can be encapsulated by any suitable encapsulating material, which includes, but is not limited to, a dendrimer, a polypeptide, an oligonucleotide, a surfactant, a small organic or inorganic molecule, a combination of several such small molecules as ligands and a non-dendrimer polymer. In one embodiment, the dendrimer is a PAMAM dendrimer.

In another embodiment, the polypeptide comprises a sequence ranging form 5-500 amino acids in length. In another embodiment, the polypeptide comprises an antibody.

[074] As used herein with respect to a dendrimer, for example, "encapsulated" means that the one or more molecules of the noble metal nanocluster can be physically associated with or entrapped within the core of the dendrimer, dispersed partially or fully throughout the dendrimer, or attached or linked to the dendrimer or any combination thereof, whereby the attachment or linkage is by means of covalent bonding, hydrogen bonding, adsorption, metallic bonding, van der Waals forces or ionic bonding, or any combination thereof. Since the size, shape and functional group density of the dendrimers can be rigorously controlled by well-known methods, there are many ways in which the carried material (i.e. the noble metal nanoclusters) can be associated with the dendrimer. For example, (a) there can be covalent, coulombic, hydrophobic, or chelation type association between the carried material(s) and entities, typically functional groups, located at or near the surface of the dendrimer; (b) there can be covalent, coulombic, hydrophobic, or chelation type association between the carried material(s) and moieties located within the interior of the dendrimer; (c) the dendrimer can be prepared to have an interior which is predominantly hollow allowing for entrapment (e.g., physically within or by association with the interior moieties of the dense star dendrimer) of the carried materials within the interior (void volume), (e.g., magnetic or paramagnetic cores or domains created by the chelation and complete or incomplete reduction of metal ions to the zero or non-zero valence state within the dendrimer), these dendrimers containing magnetic interiors can be used for harvesting various bioactive entities that can be complexed with various dendrimer surfaces by use of magnets and the like, wherein the release of the carried material can optionally be controlled by congesting the surface of the dendrimer with diffusion controlling moieties; or (d) various combinations of the aforementioned phenomena can be employed.

[075] As used herein, the term "noble metal" refers to the group of elements selected from the group consisting of gold, silver, and copper and the platinum group metals (PGM) platinum, palladium, osmium, iridium, ruthenium and rhodium. In certain preferred embodiments of the present invention, the noble metal is selected from the group consisting of gold, silver, and copper. In other preferred embodiments, the noble metal is silver. In other preferred embodiments, the noble metal is gold. In other preferred embodiments, the noble metal is copper.

[076] As used herein, the term "nanocluster" refers to an association of 2-27 atoms of a metal. Manufactured nanoclusters are known and are becoming increasingly important in the fields of catalysis, ceramics, semiconductors, and materials science, among others. Their importance is due to the high ratio of surface atoms to interior atoms in nanoclusters. This imparts properties such as high surface reactivities, increased hardness and yield, strength, decreased ductility, liquid-like behavior at low temperature, and size-related chemical, physical, and/or quantum effects that are distinct from those properties of their macro-scale counterparts. At its finest division, an element consists of a single atom. Molecules consist of simple aggregates of a few atoms, and glasses and other microcrystalline or macrocrystalline solids comprise an amorphous, crystalline or polycrystalline lattice extending outwards in continuous, three dimensional arrays of atoms. The dimensions of atoms and molecules are measured in angstroms, one angstrom being 10^{-10} m or 0.1 nanometers. Crystalline domains in microcrystalline solids such as metals typically are measured on the scale of micrometers. Nanoclusters occupy the transition from the simple atomic state to the nanocrystalline state and may have diameters in the range of about 0.1 to about 3 nm. Preferably, the nanoclusters as described herein comprise approximately 2, 3, 4, 5, 6, 7, 8, 9, 10, 11, 12, 13, 14, 15, 16, 17, 18, 19, 20, 21, 22, 23, 24, 25, 26, or 27 atoms. In other preferred embodiments, the nanoclusters comprise approximately 2-27 atoms, approximately 2-25 atoms, approximately 2-20 atoms, approximately 2-15 atoms, approximately 2-10 atoms, or approximately 2-8 atoms. The size of the nanocluster preferred for encapsulation in an encapsulating material such as a dendrimer or peptide can depend on the type of metal used, the desired emission color, and the particular application.

[077] As used herein, a "nanoparticle" is defined as a particle having a diameter of from approximately 3 to approximately 100 nanometers, having any size, shape or morphology, and comprising a noble metal as defined herein.

[078] As used herein, a "nanodot" is a noble metal nanocluster that is encapsulated in an encapsulating material, such as a dendrimer or a peptide, wherein the encapsulated noble metal nanocluster is capable of fluorescing at a low excitation intensity. In one embodiment, the encapsulated noble metal nanocluster has a fluorescence quantum yield of greater than approximately 1% and has a saturation intensity ranging from approximately 1 to 10^6 W/cm^2 at a nanocluster excitation maximum. In certain embodiments, the fluorescence quantum yield is greater than

approximately 2%, 3%, 4%, 5%, 10%, 15%, 20%, 25%, 30%, 35%, 40%, 45%, 50%, 60% or higher. In certain embodiments, the saturation intensity ranges from approximately 1-10^6 W/cm^2, from approximately 10-800 W/cm^2, from approximately 10-10,000 W/cm^2, from approximately 10-100,000 W/cm^2, from approximately 10-1,000,000 W/cm^2, or from approximately 10-500 W/cm^2. The excitation maximum varies between nanoclusters, and is dependent at least on the type of metal atom, and the number of metal atoms in the nanocluster. The excitation maximum for a nanocluster is readily determined by one of ordinary skill in the art using means that are well known in the art.

[079] As used herein, the term "saturation intensity" refers to the intensity at which the absorption of the molecule saturates and is no longer linear with respect to excitation intensity. At the saturation intensity for the non-linear absorption of a molecule, multiphoton absorption is no longer dependent on the intensity raised to the power of the non-linear interaction. The quantum yield is defined as the ratio of the number of photons emitted to the number of photons absorbed.

[080] As used herein, the term "water-soluble" refers to the ability to dissolve and/or form a suspension in an aqueous solution. While the fluorescent label may visibly dissolve in an aqueous solution, it is at least temporarily dispersible or capable of forming a suspension in an aqueous solution.

[081] As used herein, the term "fluorescence" or "fluorescent" is a physical phenomenon based upon the ability of certain molecules to absorb and emit light at different wavelengths. The absorption of light (photons) at a first wavelength is followed by the emission of photons at a second wavelength and different energy. As used herein, a "fluorescent label" is a molecule that absorbs light at a first wavelength and emits the photons at a second wavelength and different energy. As used herein, a "fluorescent label" is used interchangeably with a "luminescent label," and "fluorescent" and "fluorescence" are used interchangeably with the terms "luminescent" and "luminescence," respectively. Emission can arise from single photon or multiphoton absorption. As such, fluorescence is meant to include phosphorescence, linear fluorescence, multiphoton excited fluorescence, and all emissions indicated by the term "luminescence." As used herein, the term "saturated fluorescence" refers to a sub-linear increase in fluorescence with incident intensity. Preferably, the fluorescent label comprises an encapsulated noble metal nanocluster. Preferably, the fluorescent labels of the present invention fluoresce at a low excitation

intensity, such as that provided by a mercury lamp. Preferably, the low excitation intensity is approximately 30 W/cm^2 at approximately 460 nm. In other embodiments, the excitation intensity can range from < 1 W/cm^2 up to 10 kW/cm^2 at a range of excitation wavelengths from approximately 330 nm to approximately 1600 nm. The excitation intensity can vary depending at least on the size of the nanocluster, the metal comprising the nanocluster, and the composition of the scaffold, and can be readily determined by one of ordinary skill in the art using methods well known in the art. While the fluorescent label as described herein is capable of fluorescing at a low excitation energy such as by a weak mercury lamp, in one embodiment the fluorescent label can fluoresce when activated by a laser.

[082] Optionally, the fluorescent label may also have single molecule Raman spectra. While the examples herein focus primarily on Raman scattering, and in particular surface enhanced Raman scattering (SERS), those practiced in the art of Raman spectroscopy are aware that the general concept of inelastic light scattering has many alternative manifestations that can be used for detection. The basic "normal" Raman scattering experiment involves detection/measurement of Stokes-shifted photons, i.e., those with a lower energy than the incident photons. Anti-Stokes photons-those with energies greater than the incident photons-are also generated in a Raman experiment. While the intensity of anti-Stokes Raman bands is typically low compared to the Stokes bands, they offer one very significant advantage: the lack of interference from fluorescence, which by definition occurs at lower energies than excitation. In certain embodiments of the invention, the nanodots have single-molecule anti-Stokes spectra. As used herein, "Raman spectra" includes both Stokes and anti-Stokes bands.

[083] Practice of the invention is not limited to the instrumentation described herein: Raman experiments with nanodots can be carried out with visible or near-IR irradiation, make use of Raman bands from 300 cm^{-1} to 3300 cm^{-1}, employ any form of monochromator or spectrometer to spatially, spectrally or temporally resolve photons, and any form of photon detector.

[084] Those skilled in the art will recognize that there is a great deal of latitude in the composition of a scaffold or encapsulating material that yields a distinct Raman spectrum. The encapsulating material can also be a polymer, such as, but not limited to a dendrimer, to which one or more further Raman-active moieties are attached. In this case, differentiable nanodots contain the same polymer, but the

dendrimers may have different attached functional groups yielding different Raman spectra, or the functional groups may be located in varying positions within the dendrimer, also yielding different Raman spectra. Alternatively, one or more bands in the Raman spectrum of an functional group may be dependent on the density of the encapsulating material in the nanodot. Nanodots formed with different densities of the same encapsulating material are therefore differentiable from one another. Note that the encapsulating materials may contain functional groups amenable to molecular attachment. Thus, the encapsulating materials can be modified with all forms of biomolecules and biomolecular superstructures including cells, as well as oxides, metals, polymers, specific bonds, etc. In short, the encapsulating materials support essentially any and all forms of chemical functionalization (derivatization).

[085] As used herein, the term "target analyte" means any analyte which it is desired to detect or quantify. In this context "detect" means to establish that an analyte or class of analyte could be in a sample. Where circumstances require detection may be followed by positive identification using further confirmatory testing with complementary methods.

[086] A "sample" may be anything which it is desired to test for an analyte. In certain embodiments, the sample is a biological sample.

[087] In further embodiments, the encapsulated noble metal nanocluster has a characteristic multiphoton excitation spectra. Multiphoton excitation results from more than one photon either sequentially or simultaneously exciting a molecule (Shen, Principles of Nonlinear Optics, John Wiley & Sons, 1984). Sequential absorption of two photons (light) by molecules, for example, results in the creation of an excited molecular state with subsequent excitation from that prepared state into a third state. This process requires two photons in succession to interact with the same molecule before the intermediate state has decayed. Resulting from two sequential linear processes (i.e. each depending linearly on the incident intensity), the overall intensity dependence of the entire process is quadratic with respect to incident intensity, or depends on the square of the incident intensity (Kneipp *et al.*, J. Am. Chem. Soc. 2004, 76:2444).

[088] Vibrational energy is deposited in scaffold/nanocluster complex through an ordinary Raman scattering process, thereby producing an excited vibrational level. This excited vibrational level will typically decay to the ground vibrational state within 10-20 picoseconds (ps). If a second Raman process occurs before the excited state

decays, Anti-stokes Raman scattering can occur that produces higher energy light than that used for excitation by adding the vibrational energy to the incident laser energy. Overall, this sequential process depends on the second power of the incident laser intensity. At sufficiently low incident intensities, very weak Anti-stokes Raman scattering may be observed resulting from thermal population of excited vibrational levels. Because these are not excited by the incident laser, the Anti-stokes emission resulting from these starting levels is only linear with the incident laser intensity. Due to this combination of linear and sequential multiphoton processes, any measured incident intensity dependence exceeding linearity by more than 10% is considered non-linear or resulting from a multiphoton event, whether sequential or simultaneous. Consequently, any process with an observed signal intensity that depends on the incident intensity in a greater than linear fashion (e.g. is linearly proportional to the incident intensity raised to the power of 1.1 or greater) is to be considered a multiphoton or non-linear process (Shen, Principles of Nonlinear Optics, John Wiley & Sons, 1984). Secondary excitation from an excited electronic state would also give such a non-linear process that could be sequential in nature if the second photon interacts with the molecule in its excited electronic level.

[089] Simultaneous absorption of multiple photons results from non-linear interactions of the molecule with the excitation source. Termed non-linear optics, this simultaneous absorption of more than one photon also exhibits a greater than linear dependence on the excitation intensity. Simultaneous multiphoton excitation includes two-photon or second harmonic generation, three-photon, or third harmonic generation, and all higher order processes, as well as multiphoton excited fluorescence and all multiphoton or non-linear optical processes defined as multiphoton excitation or as resulting from multiphoton excitation. Simultaneous multiphoton absorbance does not directly populate the intermediate state of the molecule, but instead two lower energy photons combine to resonantly excite or interact with a single excited state of the molecule/nanocluster system. The non-linear polarization induced in the molecule or sample may simply generate new colors of light (harmonic generation) that result from the combination of two or more photons within the molecule to produce new colors of light (Shen, Principles of Nonlinear Optics, John Wiley & Sons, 1984). This interaction may also excite specific states within the molecule to produce multiphoton-excited fluorescence with similar or different properties from linear or ordinary fluorescence.

[090] Typically harmonic generation requires long-range interactions for sufficient build-up of signal, but it is possible to generate within small focal volumes in high resolution optical microscopes. Under such tight focusing conditions, the wavevector matching normally required for the generation of non-linear signals (e.g. harmonic generation) need not be met. This means that the non-linear signal is not directional due to the tight focusing and the signal is produced in all directions (Shen, Principles of Nonlinear Optics, John Wiley & Sons, 1984). Consequently, high sensitivity epi detection (or collection in a reflected or back-scattered geometry) can be achieved, as was demonstrated for CARS (Cheng *et al.*, J. Phys. Chem. B 2001, 105:1277-1280)and third harmonic generation microscopy (Cheng *et al.*, J. Opt. Soc. Amer. B 2002, 19:1604-1610) – another non-linear Raman-based technique. The lack of wavevector matching means that this can potentially be observed on the single molecule level if the non-linear interaction is sufficiently strong. This non-linear interaction is typically characterized by the non-linear susceptibility or the hyperpolarizability and gives rise to second harmonic generation even from seemingly symmetric structures. This non-wave vector matched doubling of light (or second harmonic generation) is often called "Hyper-Rayleigh scattering" (Shen, Principles of Nonlinear Optics, John Wiley & Sons, 1984), but has never been reported as arising from individual molecules, individual species of any type or individual sub-10 nm nanoparticles, sub-5-nm nanoparticles, sub 2-nm nanoparticles, sub1-nm nanoparticles, metal nanoclusters of any size or type, or the encapsulated nanoclusters described herein.

[091] The spectral emission can be determined for the labels of the present invention. Atoms and collections of atoms (or molecules) can make transitions between the electronic energy levels allowed by quantum mechanics by absorbing or emitting the energy difference between the levels. The wavelength of the emitted or absorbed light is such that the photon carries the energy difference between the two states. This energy may be calculated by dividing the product of the Planck constant and the speed of light hc by the wavelength of the light. Thus, an atom or collection of atoms can absorb or emit only certain wavelengths (or equivalently, frequencies or energies) as dictated by the detailed atomic structure of the atoms and their combinations upon chemical interaction. When the corresponding light is passed through a prism or spectrograph it is separated spatially according to wavelength. The corresponding spectrum may exhibit a continuum, or may have superposed on the

continuum bright lines (an emission spectrum). Thus, emission spectra are produced when the atoms do not experience many collisions (because of the low density). The emission lines correspond to photons that are emitted when excited states in the molecule or collection of atoms make transitions back to lower-lying levels. In a preferred embodiment of the present invention, the spectral emission of the fluorescent label is polarized. In other embodiments, depending on nanocluster properties, the emission may exhibit different degrees of polarization. In certain embodiments, the encapsulated noble metal nanocluster exhibits a dipole emission pattern. Preferably, the spectral emission characteristics of the fluorescent label are at least partially determined by one or more characteristics selected from the group consisting of: the encapsulating material used, the generation of the dendrimer, the pH of the test environment, the pH of the environment in which the nanodot is formed, the affinity of the peptide for the noble metal nanocluster which is determined by the peptide sequence, the size of the nanocluster, and the specific noble metal used to form the encapsulated noble metal nanocluster.

[092] Preferably the noble metal nanocluster has a varying charge. As used herein, the term "varying charge" refers to the fact that a noble metal nanocluster can be completely or incompletely reduced, can be neutral, or can be negatively charged. In certain applications, a noble metal nanocluster of a certain charge may be preferred. The charge of a noble metal nanocluster is readily determined by one of ordinary skill in the art using well-known methods.

[093] The noble metal nanoclusters of the present invention are preferably less than 3 nm in diameter, and can be smaller than 2 nm or 1 nm in diameter. After encapsulation, the encapsulated noble metal nanoclusters can range in diameter from less than 1 nm to approximately or greater than 15 nm. The size of the encapsulated noble metal nanocluster is largely dependent on the encapsulating material used. For example, in one embodiment, an antibody such as IgG is used to encapsulate the noble metal nanocluster. These antibodies are approximately 10 nm in diameter. Large 10-50 nm encapsulated noble metal nanoclusters can be filtered by the lymphatic system *in vivo* for imaging purposes.

[094] As used herein, a "dendritic polymer" is a polymer exhibiting regular dendritic branching, formed by the sequential or generational addition of branched layers to or from a core. The term dendritic polymer encompasses "dendrimers," which are characterized by a core, at least one interior branched layer, and a surface

branched layer. (See Dvornic & Tomalia in Chem. in Britain, 641-645, August 1994.) A "dendron" is a species of dendrimer having branches emanating from a focal point which is or can be joined to a core, either directly or through a linking moiety to form a dendrimer. Many dendrimers comprise two or more dendrons joined to a common core. However, the term dendrimer is used broadly to encompass a single dendron. In the present invention, a preferred dendrimer is a poly(amidoamine) or PAMAM dendrimer, however, the use of other dendrimers is contemplated. The dendrimer may be selected from the group consisting of a 0^{th} generation, a 1^{st} generation, a 2^{nd} generation, a 3^{rd} generation, a 4^{th} generation or greater generation dendrimer. The dendrimer can have any termination, including, but not limited to a OH terminating, COOH terminating, and NH_2 terminating. The generation of the dendrimer selected varies depending on the desired specific application for the encapsulated noble metal nanocluster.

[095] Dendritic polymers include, but are not limited to, symmetrical and unsymmetrical branching dendrimers, cascade molecules, arborols, and the like, though the most preferred dendritic polymers are dense star polymers. The PAMAM dendrimers disclosed herein are symmetric, in that the branch arms are of equal length. The branching occurs at the hydrogen atoms of a terminal -NH2 group on a preceding generation branch.

[096] Even though not formed by regular sequential addition of branched layers, hyperbranched polymers, e.g., hyperbranched polyols, may be equivalent to a dendritic polymer where the branching pattern exhibits a degree of regularity approaching that of a dendrimer.

[097] Topological polymers, with size and shape controlled domains, are dendrimers that are associated with each other (as an example covalently bridged or through other association as defined hereafter) through their reactive terminal groups, which are referred to as "bridged dendrimers." When more than two dense star dendrimers are associated together, they are referred to as "aggregates" or "dense star aggregates."

[098] Therefore, dendritic polymers include bridged dendrimers and dendrimer aggregates. Dendritic polymers encompass both generationally monodisperse and generationally polydisperse solutions of dendrimers. The dendrimers in a monodisperse solution are substantially all of the same generation, and

hence of uniform size and shape. The dendrimers in a polydisperse solution comprise a distribution of different generation dendrimers.

[099] Dendritic polymers also encompass surface modified dendrimers. For example, the surface of a PAMAM dendrimer may be modified by the addition of an amino acid (e.g., lysine or arginine).

[0100] As used herein, the term "generation" when referring to a dendrimer means the number of layers of repeating units that are added to the initiator core of the dendrimer. For example, a 1st generation dendrimer comprises an initiator core and one layer of the repeating unit, and a 2nd generation dendrimer comprises an initiator core and two layers of the repeating unit, etc. Sequential building of generations (i.e., generation number and the size and nature of the repeating units) determines the dimensions of the dendrimers and the nature of their interior.

[0101] Methods for linking dendrimers to biological substrates are well known to those of skill in the art, and include the use of linker molecules. For example, thiol-reactive species can be made by coupling the dendrimer hydroxyl group to the isocyanate end of the bi-functional cross-linker, N-(p-maleimidophenyl)isocyanate, leaving a thiol-reactive maleimide for coupling to proteins.

[0102] As used herein, the term "photobleaching" comprises all processes, which result in the reduction of the intensity of fluorescent light generated at the wavelength of excitation. In embodiments of the present invention, the noble metal nanocluster emits greater than approximately 10^6, 10^7, 10^8, 10^9, 10^{10}, or 10^{11} photons before photobleaching. In a more preferred embodiment, the noble metal nanocluster emits greater than approximately 10^{12} photons before photobleaching. Photobleaching is readily assessed by one of ordinary skill in the art.

[0103] In certain embodiments of the present invention, when the encapsulated noble metal nanoclusters are excited, greater than approximately 80% of the noble metal nanoclusters fluoresce for greater than approximately 30 minutes. In further embodiments, the noble metal nanoclusters fluoresce at a continuous excitation energy of approximately 300 W/cm^2 at 514.5 nm or 476 nm. In another embodiment, greater than approximately 90% of the noble metal nanoclusters fluoresce for greater than approximately 30 minutes. In other embodiments, greater than 80%, or greater than 90% of the nanoclusters have a fluorescence quantum yield of greater than approximately 1% and a saturation intensity that ranges from 1-10^6 W/cm^2 with emission continuing for greater than 30 minutes.

[0104] In one embodiment, a dendrimer encapsulated noble metal nanocluster is used to deliver noble metal nanoclusters across biological membranes to a peptide that strongly binds the noble metal nanocluster. The strength of binding to the noble metal nanocluster is readily determined by one of ordinary skill in the art, and can include a visual estimation of the intensity of the fluorescence, second or higher harmonic signal, or intensity of the bands of the Raman spectra. In a preferred embodiment, the dendrimer is a lower generation dendrimer, such as a 0^{th} generation, 1^{st} generation, or 2^{nd} generation. In other embodiments, the dendrimer is a higher generation dendrimer, such as a 3^{rd} or 4^{th} or higher generation dendrimer. In certain embodiments, the peptide binds the noble metal nanocluster at a range of pH. In other embodiments, the peptide stably binds the noble metal nanocluster at a pH range of between 10 and 1, more preferably between 9 and 2, more preferably between 8 and 3. In other embodiments the peptide stably binds the noble metal nanocluster at a pH of 9, 8, 7, 6, 5, 4, or 3. This embodiment will allow for the facile labeling of proteins both *in vitro* and *in vivo*.

[0105] In certain embodiments of the foregoing, an oligonucleotide encapsulates the noble metal nanocluster. The terms "polynucleotide," "oligonucleotide," "nucleic acid" and "nucleic acid molecule" are used herein to include a polymeric form of nucleotides of any length, either ribonucleotides or deoxyribonucleotides. This term refers only to the primary structure of the molecule; thus, the term includes triple-, double- and single-stranded DNA, as well as triple-, double- and single-stranded RNA. It also includes modifications, such as by methylation and/or by capping, and unmodified forms of the polynucleotide. More particularly, the terms "polynucleotide," "oligonucleotide," "nucleic acid" and "nucleic acid molecule" include polydeoxyribonucleotides (containing 2-deoxy-D-ribose), polyribonucleotides (containing D-ribose), any other type of polynucleotide which is an N- or C-glycoside of a purine or pyrimidine base, and other polymers containing non-nucleotidic backbones, for example, polyamide (e.g., peptide nucleic acids (PNAs)) and polymorpholino (commercially available from the Anti-Virals, Inc., Corvallis, Ore., as Neugene) polymers, and other synthetic sequence-specific nucleic acid polymers providing that the polymers contain nucleobases in a configuration which allows for base pairing and base stacking, such as is found in DNA and RNA. In certain embodiments, the oligonucleotide is or comprises an oligonucleotide selected from the group consisting of SEQ ID NOs: 2, 3, 4, 5, 6, 7, and 8.

[0106] There is no intended distinction in length between the terms "polynucleotide," "oligonucleotide," "nucleic acid" and "nucleic acid molecule," and these terms will be used interchangeably. These terms refer only to the primary structure of the molecule. Thus, these terms include, for example, 3′-deoxy-2′, 5′-DNA, oligodeoxyribonucleotide N3′ P5′ phosphoramidates, 2′-O-alkyl-substituted RNA, double- and single-stranded DNA, as well as double- and single-stranded RNA, DNA:RNA hybrids, and hybrids between PNAs and DNA or RNA, and also include known types of modifications, for example, labels which are known in the art, methylation, "caps," substitution of one or more of the naturally occurring nucleotides with an analog, internucleotide modifications such as, for example, those with uncharged linkages (e.g., methyl phosphonates, phosphotriesters, phosphoramidates, carbamates, etc.), with negatively charged linkages (e.g., phosphorothioates, phosphorodithioates, etc.), and with positively charged linkages (e.g., aminoalklyphosphoramidates, aminoalkylphosphotriesters), those containing pendant moieties, such as, for example, proteins (including nucleases, toxins, antibodies, signal peptides, poly-L-lysine, etc.), those with intercalators (e.g., acridine, psoralen, etc.), those containing chelators (e.g., metals, radioactive metals, boron, oxidative metals, etc.), those containing alkylators, those with modified linkages (e.g., alpha anomeric nucleic acids, etc.), as well as unmodified forms of the polynucleotide or oligonucleotide. In particular, DNA is deoxyribonucleic acid.

[0107] These terms also encompass untranslated sequence located at both the 3' and 5' ends of the coding region of the gene: at least about 1000 nucleotides of sequence upstream from the 5' end of the coding region and at least about 200 nucleotides of sequence downstream from the 3' end of the coding region of the gene. Less common bases, such as inosine, 5-methylcytosine, 6-methyladenine, hypoxanthine and others can also be used for antisense, dsRNA and ribozyme pairing. For example, polynucleotides that contain C-5 propyne analogues of uridine and cytidine have been shown to bind RNA with high affinity and to be potent antisense inhibitors of gene expression. Other modifications, such as modification to the phosphodiester backbone, or the 2'-hydroxy in the ribose sugar group of the RNA can also be made. The antisense polynucleotides and ribozymes can consist entirely of ribonucleotides, or can contain mixed ribonucleotides and deoxyribonucleotides. The polynucleotides of the invention may be produced by any means, including genomic

preparations, cDNA preparations, in vitro synthesis, RT-PCR, and *in vitro* or *in vivo* transcription.

[0108] An "isolated" nucleic acid molecule is one that is substantially separated from other nucleic acid molecules that are present in the natural source of the nucleic acid (i.e., sequences encoding other polypeptides). Preferably, an "isolated" nucleic acid is free of some of the sequences that naturally flank the nucleic acid (i.e., sequences located at the 5' and 3' ends of the nucleic acid) in its naturally occurring replicon. For example, a cloned nucleic acid is considered isolated. A nucleic acid is also considered isolated if it has been altered by human intervention, or placed in a locus or location that is not its natural site, or if it is introduced into a cell by transfection. Moreover, an "isolated" nucleic acid molecule can be free from some of the other cellular material with which it is naturally associated, or culture medium when produced by recombinant techniques, or chemical precursors or other chemicals when chemically synthesized.

[0109] Specifically excluded from the definition of "isolated nucleic acids" are: naturally–occurring chromosomes (such as chromosome spreads), artificial chromosome libraries, genomic libraries, and cDNA libraries that exist either as an *in vitro* nucleic acid preparation or as a transfected/transformed host cell preparation, wherein the host cells are either an *in vitro* heterogeneous preparation or plated as a heterogeneous population of single colonies. Also specifically excluded are the above libraries wherein a specified nucleic acid makes up less than 5% of the number of nucleic acid inserts in the vector molecules. Further specifically excluded are whole cell genomic DNA or whole cell RNA preparations (including whole cell preparations that are mechanically sheared or enzymatically digested). Even further specifically excluded are the whole cell preparations found as either an *in vitro* preparation or as a heterogeneous mixture separated by electrophoresis wherein the nucleic acid of the invention has not further been separated from the heterologous nucleic acids in the electrophoresis medium (e.g., further separating by excising a single band from a heterogeneous band population in an agarose gel or nylon blot).

[0110] In one preferred embodiment, an isolated nucleic acid encoding a peptide that binds a noble metal nanocluster is introduced into a cell, and the peptide is expressed and binds the noble metal nanocluster. In certain embodiments, isolated nucleic acids encoding a peptide that binds the noble metal nanocluster can also be chimeric or fusion polynucleotides. As used herein, a "chimeric polynucleotide" or

"fusion polynucleotide" comprises a nucleic acid encoding a peptide that binds the noble metal nanocluster operably linked to a second nucleic acid sequence. Preferably, the second nucleic acid sequence encodes a protein that does not bind or does not strongly bind the noble metal nanocluster, and has both a different polynucleotide sequence and encodes a protein having a different function than a nucleic acid encoding a peptide that binds the noble metal nanocluster. Within the fusion polynucleotide, the term "operably linked" is intended to indicate that the nucleic acid encoding a peptide that binds the noble metal nanocluster and the second nucleic acid sequence, respectively, are fused to each other so that both sequences fulfill the proposed function attributed to the sequence used. The second nucleic acid sequence can be fused to the N-terminus or C-terminus of the nucleic acid encoding a peptide that binds the noble metal nanocluster.

[0111] Procedures for introducing a nucleic acid into a cell are well known to those of ordinary skill in the art, and include, without limitation, transfection, transformation or transduction, electroporation, particle bombardment, agroinfection, and the like. In certain embodiments, the nucleic acid is incorporated into a vector or expression cassette that is then introduced into the cell. Other suitable methods for introducing nucleic acids into host cells can be found in Sambrook, *et al.*, *Molecular Cloning: A Laboratory Manual*. 2nd Ed., Cold Spring Harbor Laboratory, Cold Spring Harbor Laboratory Press, Cold Spring Harbor, NY, 1989, and other laboratory manuals such as *Methods in Molecular Biology*, 1995, Vol. 44, *Agrobacterium protocols*, Ed: Gartland and Davey, Humana Press, Totowa, New Jersey.

[0112] As used herein, the term polypeptide refers to a chain of at least four amino acids joined by peptide bonds. The chain may be linear, branched, circular or combinations thereof. The terms "peptide," "polypeptide," and "protein" are used interchangeably herein. The terms do not refer to a specific length of the product. Thus, "peptides," "oligopeptides," and "proteins" are included within the definition of polypeptide. The terms include post-translational modifications of the polypeptide, for example, glycosylations, acetylations, phosphorylations and the like. In addition, protein fragments, analogs, mutated or variant proteins, fusion proteins and the like are included within the meaning of polypeptide.

[0113] The invention also provides chimeric or fusion polypeptides. As used herein, an "chimeric polypeptide" or "fusion polypeptide" comprises an polypeptide which binds a noble metal nanocluster operatively linked to a second polypeptide.

Preferably the second polypeptide has an amino acid sequence that is not substantially identical to a noble metal nanocluster optimized binding polypeptide, e.g., a polypeptide which does not stably bind a noble metal nanocluster as described herein. As used herein with respect to the fusion polypeptide, the term "operatively linked" is intended to indicate that the two polypeptides are fused to each other so that both sequences fulfill the proposed function attributed to the sequence used. The second polypeptide can be fused to the N-terminus or C-terminus of the polypeptide which binds a noble metal nanocluster. Such fusion polypeptides can facilitate the single molecule or bulk studies and allow for the direct labeling of peptides *in vivo* or *in vitro*.

[0114] In certain embodiments of the present invention, the peptide which binds the noble metal nanocluster is from approximately 5-1000 amino acids in length, from 1-800 amino acids in length, or from 5-500 amino acids in length. In certain embodiments, the peptide is from approximately 5-10 amino acids in length. In other embodiments, the peptide is from approximately 10-20 or from 20-40 amino acids in length. In one embodiment, the peptide comprises a polypeptide sequence as defined in SEQ ID NO:1.

[0115] The present invention further encompasses methods for the preparation of the encapsulated noble metal nanoclusters having the characteristics as described herein. In one embodiment, the method of preparing a dendrimer encapsulated noble metal nanocluster comprises the steps of: a) combining a dendrimer, an aqueous solution comprising a noble metal, and an aqueous solvent to create a combined solution; b) adding a reducing agent; c) subsequently adding a sufficient amount of an acidic compound to adjust the combined solution to a neutral range pH; and d) mixing the pH adjusted, combined solution to allow the formation of a dendrimer encapsulated noble metal nanocluster. In a second embodiment, the method of preparing a peptide encapsulated noble metal nanocluster capable of fluorescing comprises the steps of: a) combining a peptide, an aqueous solution comprising a noble metal, and distilled water to create a combined solution; b) adding a reducing agent; c) subsequently adding a sufficient amount of an acidic compound to adjust the combined solution to a neutral range pH; and d) mixing the pH adjusted, combined solution to allow the formation of the peptide encapsulated noble metal nanocluster. In a third embodiment, the method of preparing an oligonucleotide encapsulated noble metal nanocluster capable of fluorescing comprises the steps of: a) combining an oligonucleotide, an aqueous solution comprising a noble metal, and distilled water to create a combined

solution; b) adding a reducing agent; c) subsequently adding a sufficient amount of an acidic compound to adjust the combined solution to a neutral range pH; and d) mixing the pH adjusted, combined solution to allow the formation of the oligonucleotide encapsulated noble metal nanocluster. In further embodiments, the reducing agent is a chemical or photochemical reducing agent.

[0116] In these methods, a reducing agent is added to the combined solution to photoactivate the noble metal nanoclusters. Preferably the reducing agent is selected from the group comprising a chemical reducing agent, light, or a combination thereof. In certain embodiments of these methods, light can be used as a reducing agent to photoactivate the noble metal nanoclusters. In certain other embodiments of these methods, a chemical reducing agent can be used as a reducing agent. In one embodiment, light is used in combination with a reducing agent to photoactivate the noble metal nanoclusters. Preferably the process of preparing the encapsulated noble metal nanoclusters is performed at a temperature of between approximately 65°F to approximately 100°F. More preferably, the temperature of the combined solution from steps a) through c) is between approximately 68°F to approximately 80°F, and even more preferably between approximately 68°F to approximately 74°F.

[0117] Preferably, the aqueous solution comprising a noble metal used in the preparation of the compounds is selected from the group consisting of $AgNO_3$, $HAuCl_4 \cdot nH_2O$, and $CuSO_4 \cdot nH_2O$. In one embodiment, the aqueous solution comprising a noble metal is $AgNO_3$. In another embodiment, the aqueous solution comprising a noble metal is $HAuCl_4 \cdot nH_2O$. In a further embodiment, the aqueous solution comprising a noble metal is $CuSO_4 \cdot nH_2O$.

[0118] In one embodiment, the aqueous solution comprising a noble metal is $HAuCl_4 \cdot nH_2O$, a reducing agent is added to the combined solution, and the pH adjusted, combined solution is mixed for at least one hour to allow the formation of the dendrimer encapsulated gold nanocluster. In another embodiment, the pH adjusted, combined solution is mixed for about 48 hours to allow the formation of a dendrimer encapsulated gold nanocluster. In another embodiment, encapsulated noble metal nanoclusters are created through photoreduction through irradiation with visible or ultraviolet light to allow the formation of a dendrimer encapsulated gold, silver or copper nanocluster.

[0119] In another embodiment, when the encapsulating material is a peptide, preferably the noble metal to peptide molar ratio in step a) is approximately 0.1:1. In another embodiment, the noble metal to peptide molar ratio in step a) is less than approximately 0.1:1, and in other embodiments it is greater than 0.1:1, and can be 1:1 or greater.

[0120] In certain embodiments, the encapsulated noble metal nanocluster label is present in a biological sample. In certain preferred embodiments, the peptide or oligonucleotide which encapsulates the noble metal nanocluster is expressed within a cell, also termed "genetically programmed." As used herein, the term "expressed" encompasses the transcription and/or the translation of the peptide. In other embodiments, the peptide or oligonucleotide encapsulating the noble metal nanocluster is introduced into a biological sample. As used herein, a "biological sample" refers to a sample of isolated cells, tissue or fluid, including but not limited to, for example, plasma, serum, spinal fluid, semen, lymph fluid, the external sections of the skin, respiratory, intestinal, and genitourinary tracts, tears, saliva, milk, blood cells, tumors, organs, and also samples of *in vitro* cell culture constituents (including, but not limited to, conditioned medium resulting from the growth of cells in cell culture medium, putatively virally infected cells, recombinant cells, and cell components). The fluorescent labels can be used in a cell from any type of organism, wherein the organism is a prokaryote or a eukaryote. In preferred embodiments of the present invention, the organism is a eukaryote. Non-limiting examples of the eukaryotic cells of the present invention include cells from animals, plants, fungi, protists, and other microorganisms. In certain embodiments, the cells are part of a multicellular organism, *e.g.*, a plant or animal.

[0121] As discussed herein, the selection of the composition of the encapsulated nanocluster, as well as the size of the dendrimer or the sequence of the peptide, affects the characteristic spectral emission wavelength of the semiconductor nanocrystal. Thus, as one of ordinary skill in the art will realize, a particular composition of a nanodot as described herein will be selected based upon the spectral region being monitored. For example, nanodots that emit energy in the visible range, or in the red, blue or near-IR range can be designed. In one embodiment, the encapsulated noble metal nanocluster displays increasingly higher energy emission with decreasing nanocluster size.

[0122] The water-soluble encapsulated noble metal nanoclusters of the present invention find use in a variety of assays where other, less reliable, labeling methods have typically been used, including, without limitation, fluorescence microscopy, histology, cytology, pathology, flow cytometry, FISH and other nucleic acid hybridization assays, signal amplification assays, DNA and protein sequencing, immunoassays such as competitive binding assays and ELISAs, immunohistochemical analysis, protein and nucleic acid separation, homogeneous assays, multiplexing, high throughput screening, chromosome karyotyping, and the like. The above-described encapsulated noble metal nanocluster fluorescent labels can be used in any reporter molecule-based assay with an acceptable environment.

[0123] In certain preferred embodiments, the encapsulated noble metal nanocluster label of the present invention is used in single or bulk molecule studies. The invention encompasses methods of monitoring a molecule of interest comprising: a) attaching a water-soluble label comprising an encapsulated noble metal nanocluster to a molecule of interest, wherein the label emits an emission spectrum; and b) detecting the emission spectrum of the fluorescent label. As used herein, detecting the emission spectrum encompasses determining the optical emission properties of the label. Single molecule studies can allow for the determination of aspects of the local environment, ranging from signal strength, orientation, and lifetime, to the emission spectrum of the molecule and the degree of energy transfer with neighboring molecules. Single molecule studies have been used to manipulate individual molecules and to measure the force generated by molecular motors or covalent bonds. The development of new probe technologies allows for real-time observations of molecular interactions and trafficking within living cells. These tools allow individual members of a population to be examined, identified, and quantitatively compared within cellular sub-populations and substructures. Single molecule studies have the potential to provide spatial and temporal information that is impossible to obtain using other, more static techniques. Single molecule studies allow for measurements to be made on the *in vivo* dynamic movements of single molecules in intracellular space or to observe the behavior of single molecules over extended periods of time. Using single molecule methods, it is possible to study time trajectories and reaction pathways of individual members in a cellular assembly without averaging across populations. Cellular processes, such as exocytosis, flux through channels, or the assembly of transcription complexes, could be visualized. Individual differences in structure or function

generated by allelic polymorphisms are detectable at the level of the single molecule. Additionally, monitoring the coordinated expression of a gene or group of genes in specific tissues, or at certain developmental stages, can be performed using these technologies. As such, the use of an encapsulated noble metal nanocluster fluorescent probe allows for the determination of a spectral emission that provides information about a biological state. As used herein, the term "biological state" refers to making a determination of condition such as a quantitative and qualitative presence of a biological moiety; structure, composition, and conformation of a biological moiety; localization of a biological moiety in an environment; an interaction between biological moieties, an alteration in structure of a biological compound, and an alteration in a cellular process.

[0124] The methods and compositions of the present invention can further comprise the use of a linker molecule wherein the linker molecule is capable of attaching the fluorescent label comprising an encapsulated noble metal nanocluster to a molecule of interest.

[0125] Standard techniques for cloning, DNA isolation, amplification and purification, for enzymatic reactions involving DNA ligase, DNA polymerase, restriction endonucleases and the like, and various separation techniques are those known and commonly employed by those skilled in the art. A number of standard techniques are described in Sambrook *et al.*, 1989 Molecular Cloning, Second Edition, Cold Spring Harbor Laboratory, Plainview, New York; Maniatis *et al.*, 1982 Molecular Cloning, Cold Spring Harbor Laboratory, Plainview, New York; Wu (ed.) 1993 Meth. Enzymol. 218, Part I; Wu (ed.) 1979 Meth Enzymol. 68; Wu *et al.*, (Eds.) 1983 Meth. Enzymol. 100 and 101; Grossman & Moldave (Eds.) 1980 Meth. Enzymol. 65; Miller (ed.) 1972 Experiments in Molecular Genetics, Cold Spring Harbor Laboratory, Cold Spring Harbor, New York; Old and Primrose, 1981 Principles of Gene Manipulation, University of California Press, Berkeley; Schleif & Wensink, 1982 Practical Methods in Molecular Biology; Glover (ed.) 1985 DNA Cloning Vol. I and II, IRL Press, Oxford, UK; Hames &Higgins (eds.) 1985 Nucleic Acid Hybridization, IRL Press, Oxford, UK; and Setlow & Hollaender 1979 Genetic Engineering: Principles and Methods, Vols. 1-4, Plenum Press, New York. Abbreviations and nomenclature, where employed, are deemed standard in the field and commonly used in professional journals such as those cited herein.

[0126] Throughout this application, various publications are referenced. The disclosures of all of these publications and those references cited within those publications in their entireties are hereby incorporated by reference into this application in order to more fully describe the state of the art to which this invention pertains. In addition, the disclosures of U.S. Provisional application No. 60/551,816 and PCT/US03/20567 are hereby incorporated by reference in their entirety. The following examples are not intended to limit the scope of the claims to the invention, but are rather intended to be exemplary of certain embodiments. Any variations in the exemplified methods that occur to the skilled artisan are intended to fall within the scope of the present invention.

EXAMPLES

Example 1

Generation of dendrite- encapsulated silver nanoclusters

Methods

[0127] PAMAM is known to sequester metal ions from solution (Crooks *et al.*, Accounts Chem. Res. 2001, 34:181; Ottaviani *et al.*, Macromolecules 2002, 35:5105; Zheng *et al.*, J. Phys. Chem. B 2002, 106:1252; Varnavski *et al.*, J. Chem. Phys. 2001, 114:1962). PAMAM G4-OH and G2-OH dendrimers (4^{th}- and 2^{nd}-generation OH-terminated poly(amidoamine), respectively, Aldrich) were therefore utilized to concentrate, stabilize, and solubilize Ag nanoclusters in both aerated and deaerated aqueous solutions. By dissolving 0.5 μmol G4-OH and 1.5 μmol $AgNO_3$ into 1 ml distilled water (18 MΩ) and adjusting the solution to neutrality with 160 μmol acetic acid, silver ions readily interact with the dendrimer. Usually used to create small nanoparticles (>3 nm diameter), literature preparations generally add small amounts of reducing agents such as $NaBH_4$ (Crooks *et al.*, Accounts Chem. Res. 2001, 34:181; Ottaviani *et al.*, Macromolecules 2002, 35:5105; Zheng *et al.*, J. Phys. Chem. B 2002, 106:1252; Varnavski *et al.*, J. Chem. Phys. 2001, 114:1962). In order to create dendrimer-encapsulated nanoclusters ("nanodots"), not nanoparticles, harsh chemical reducing agents were not added to the reactions. The fluorescence of these solutions was probed by placing a 10-ml drop of the solution on a clean coverslip in ambient air, nitrogen, and/or evacuated (10-5 torr) environments which was then irradiated with blue light (450-480 nm)

from a bandpass-filtered mercury lamp through a standard epifluorescence microscope. Results were unaffected by degree of oxygenation or dendrimer generation. Alternatively, higher concentrations of Ag nanoclusters can be prepared through the addition of a photochemical reducing agent (i.e. a photoreductant) such as 9-ethyl-carbazole and blue or ultraviolet irradiation.

Results

[0128] Initially, no visible absorption or fluorescence was observed from these solutions, but, photoactivation was clearly demonstrated by the solution absorption spectra (Fig. 1A) before and after exposure to white light. Initially only the dendrimer contributed to the spectrum with a single absorption at 284 nm. After photoactivation, the solution exhibited two new peaks at 345 nm and 430 nm due to the absorption of small, photoreduced silver nanodots (Ag_2-Ag_8) (Rabin *et al.*, G. Chem. Phys. Lett. 1999, 312:394; Bonacic′-Koutecky *et al.*, J. Chem. Phys. 2001, 115:10450). The size and geometry differences of the small silver nanodots simultaneously created during photoactivation yielded multicolored fluorescence throughout the visible region. Silver nanoclusters of this size are the only ones known to have strong visible absorption and emission (Rabin *et al.*, G. Chem. Phys. Lett. 1999, 312:394; Bonacic′-Koutecky *et al.*, J. Chem. Phys. 2001, 115:10450; Linnert *et al.*, J. Am. Chem. Soc. 1990, 112:4657; Mostafavi *et al.*, Chem. Phys. Lett. 1990, 167:193). The small size was confirmed by mass spectrometry of photoactivated fluorescent nanodot solutions (Fig. 1B). Borohydride-reduced solutions yielded larger silver nanoparticles (3-7 nm) with a characteristic strong surface plasmon absorption at 398 nm, but with essentially no fluorescence (Fig. 1A). Thus, since the fluorescent silver nanodots only appeared without the plasmon absorption, they must be much smaller than 3 nm, and are likely smaller than 2 nm.

[0129] Correlating with the changes in absorption, fluorescence grew with increasing irradiation time as silver ions were photoreduced inside the dendrimer host. Within ~6 seconds, the field of view was filled with individual blinking fluorescent species, with little subsequent photoactivation (Figs. 2A-D). These very bright, stable fluorescent features were all highly polarized and exhibited well-defined dipole emission patterns (Fig. 2E; Bartko & Dickson, J. Phys. Chem. B 1999, 103:11237) and blinking dynamics (Lu *et al.*, Science 1998, 282:1877; Dickson *et al.*, Nature 1997, 388:355; Hu *et al.*, J. Am. Chem. Soc. 1999, 121:6936) characteristic of individual emitters. After completion of photoactivation in this silver-limited environment, the

fluorescent silver – dendrimer nanodots remained very stable both in average emission intensity and in spectral characteristics. The dendrimer thereby stabilized the nanoclusters and enhanced their optical properties relative to those on AgO films (Peyser *et al.*, Science 2001, 291:103; Peyser *et al.*, J. Phys. Chem. B 2002, 106:7725). Because the binding energy of small Ag nanoclusters is less than the excitation energy, the cage effect of the dendrimer likely acts similarly to that of rare gas matrices (Rabin *et al.*, Chem. Phys. Lett. 1999, 312:394) to stabilize and enhance nanocluster fluorescence by preventing photodissociation. While water is known to quench Ag nanocluster fluorescence on AgO films (Mihalcea *et al.*, J. Am. Chem. Soc. 2001, 123:7172), dendrimer-encapsulated silver nanodots were highly fluorescent and quite stable in water solution. Thus, the photochemically produced Ag nanoclusters were also protected inside the dendrimer, thereby preventing interaction with quenchers in solution.

[0130] Electrospray ionization mass spectrometry (ESI-MS) of the photoactivated nanodot solutions showed strong enrichment of dendrimer + Ag_n with n = 2-4 over non-photoactivated, and therefore non-fluorescent nanodot solutions (Fig. 1B). In non-photoactivated nanodot solutions, the dendrimer + Ag_2 and larger nanocluster peaks were unobservable, clearly indicating emission from dendrimer-encapsulated Ag nanoclusters ranging in size from 2 to at most 8 atoms once the solutions are photoactivated (Zheng & Dickson, J. Am. Chem. Soc., 2002, 124:13982-13983).

[0131] Contrary to studying nanoclusters on AgO films (Peyser *et al.*, Science 2001, 291:103; Peyser *et al.*, J. Phys. Chem. B 2002, 106:7725), single nanocluster spectroscopy was readily performed on these soluble dendrimer-encapsulated silver nanodots. While the bulk spectra of Ag_n on AgO and of the aqueous nanodot solutions (Fig. 3) was indistinguishable, individual Ag nanodots had much narrower and more stable emission spectra than either bulk nanodot samples or individual nanoclusters on AgO films (Fig. 3). Because nanocluster size on AgO films was continually modified with excitation, individual nanoclusters were observed to exhibit large spectral shifts (Peyser *et al.*, Science 2001, 291:103; Peyser *et al.*, J. Phys. Chem. B 2002, 106:7725). In contrast, five stable and easily distinguished fluorescence spectra were obtained from these highly dispersed dendrimer-encapsulated silver nanodots (Fig. 3), suggesting that the bulk spectrum was dominated by as few as five nanocluster sizes. Considerably narrower than those of bulk nanodot films or solutions, room temperature single nanodot fluorescence spectra exhibited no obvious spectral diffusion. Because

no additional silver could be incorporated into the nanodot and the dendrimer stabilized the nanodot fluorescence, single nanodot emission was quite stable and robust with maxima at 533 nm, 553nm, 589nm, 611nm and 648nm, although fluorescence intermittency was readily observed. In comparison to II-VI nanoparticles, these nanodots were very photostable with ~80% of individual features remaining fluorescent for >30 minutes of continuous 514.5 nm or 476 nm excitation at 300W/cm^2. The nanodot photoactivation, blinking, dipole emission patterns, spectral stability, mass spectrometry, and fluorescence was observed only for small sized nanodots, further confirming that individual dendrimer-encapsulated Ag_n nanoclusters less than 8 atoms in size gave rise to the observed emission. No fluorescence was observed in similarly prepared solutions without the dendrimer or solutions prepared without the silver. Crucial to solubility and stabilization, the dendrimer enhouses and protects the nanoclusters, yielding strong emission and providing a silver-limited environment that prevents further photoreduction/ nanocluster growth.

[0132] Through these methods, very photostable, water-soluble silver nanodots have been successfully created in dendrimers through direct photoreduction in ambient conditions. Such silver nanodots are quite stable and highly fluorescent both in aqueous solutions and in films and are readily observed on the single molecule level with weak mercury lamp excitation (30 W/cm^2). With synthetic control of dendrimer attachment (for example, thiol-reactive species can be made by coupling the dendrimer hydroxyl group to the isocyanate end of the bi-functional cross-linker, N-(p-maleimidophenyl)isocyanate, leaving a thiol-reactive maleimide for coupling to proteins), such simple nanomaterials are likely to find use as biological labels, thereby making single molecule studies much more widely accessible without expensive laser sources. The intense photoactivated emission and very long life before photobleaching makes these attractive new nanomaterials for studying chemical and biological systems.

Example 2

Characterization of individual Ag nanodots

[0133] A range of PAMAM dendrimer generations (G0-OH through G4-OH with diameters (MW) ranging from 1.5 nm (517g/mol) to 4.5 nm (14,215 g/mol) were used to yield highly fluorescent Ag_n nanodots. Very bright fluorescence was observed

over a pH range of 8.0 to 3.0. These different generations of PAMAM allowed a measure of control over nanocluster distributions: nanodots created with smaller dendrimer generations exhibited different emission spectra than nanodots created with higher dendrimer generations. Not only was nanodot emission extremely stable in spectrum and intensity, but they also exhibited highly polarized emission with very clear and stable dipole emission patterns (Figure 2E). The observation of emission patterns allowed the employment of the three-dimensional orientational methods developed to follow orientational dynamics either in solution or of immobilized features, as described in Bartko, & Dickson, J. Phys. Chem. B 1999, 103:3053-3056; Bartko & Dickson, J. Phys. Chem. B 1999, 103:11237-11241; and Bartko *et al.*, Chem. Phys. Lett. 2002, 358:459-465.

[0134] The photophysical parameters of many of these individual Ag nanodots have also been characterized (Fig. 4A). While much smaller than quantum dots, the extremely bright nanodot fluorescence at low excitation intensities (30W/cm^2 at 460 nm, close to the 450-nm excitation maximum) results from the very short fluorescence lifetime. After deconvolution of the instrument response, individual nanodot lifetimes exhibited a primary sub-100 ps component (92%) as measured with time-correlated single photon counting with 400-nm excitation from a doubled Ti:sapphire laser. The nanodots also had a slower (1.6 ns) decay component. The very fast relaxation indicates a very strong connection between ground and excited states, thereby yielding a very strong transition moment from a very small (several atom) nanocluster.

[0135] The absorption cross-section of individual nanodots was measured through saturation intensity measurements (Fig. 4B). These were compared with well-characterized single DiIC$_{18}$ molecules that have well-known saturation intensities, lifetimes, and fluorescence quantum yields (Macklin *et al.*, Science 1996, 272:255-258). These experiments indicate that the Ag nanodots have absorption cross sections that are greater than 20 times stronger than the best organic dyes and nearly identical to the best CdSe quantum dots. Additionally, through comparisons of total numbers of photons absorbed by single DiI molecules and single nanodots, the lower estimates of the nanodot fluorescence quantum yields have been calculated to be at least ~30%. Additionally, these Ag nanodots exhibited at least comparable photostability to much larger II-VI quantum dots, with >90% of individual features remaining fluorescent for >>30 minutes of continuous 514.5-nm excitation at 300W/cm^2. Generally lasting for more than an hour of continuous optical excitation while emitting >10^6 photons/sec

near saturation, typical individual nanodots emit well over 10^9 photons before photobleaching. This is two orders of magnitude more total photons emitted than the best available dyes emit. Consequently these nanodots offer the opportunity to probe both the short time and long time single molecule dynamics within a wide range of biological systems.

[0136] Thus, dendrimer-encapsulated water-soluble silver nanoclusters (Ag nanodots) have been created through direct photoreduction in ambient conditions. Such silver nanodots were quite stable in both solution and films and were readily observed on the single molecule level with weak mercury lamp excitation (30 W/cm^2) when excited very close to the absorption maximum of 450 nm. With synthetic control of dendrimer attachment, such simple nanomaterials are very useful as biological labels, thereby making single molecule studies much more widely accessible without expensive laser sources. The intense photoactivated emission and very long life before photobleaching makes these attractive new nanomaterials for studying biological systems.

Example 3

Generation of dendrite- encapsulated gold nanoclusters

[0137] Previous studies have yielded fluorescent, surface passivated gold nanoclusters ranging in size from 28 atoms to smaller particles (<1.2 nm) with emission in the near IR (Link *et al.*, J. Phys. Chem. B 2002, 106:3410-3415), red (Huang & Murray, J. Phys. Chem. B 2001, 105:12498-12502), and blue (Wilcoxon *et al.*, J. Chem. Phys. 1998, 108:9137-9143), with increasingly higher energy emission with decreasing nanocluster size. Although Au nanoclusters with million-fold enhanced fluorescence quantum yields ϕ_F, relative to that of bulk gold films (Mooradian, A. Phys. Rev. Lett. 1969, 22:185-187), have been created, the 10^{-3} to 10^{-4} quantum yields and polydisperse nanoparticle size distributions have precluded them from being good fluorophores (Link *et al.*, J. Phys. Chem. B 2002, 106:3410-3415; Huang & Murray, J. Phys. Chem. B 2001, 105:12498-12502). The present invention discloses water-soluble, monodisperse, blue-emitting Au_8 nanodots that when encapsulated in and stabilized by biocompatible PAMAM dendrimers (Tomalia, Sci. Am. 1995, 272:62-66), exhibited a fluorescence quantum yield of 41±5%, a more than 100-fold improvement over other reported gold nanoclusters (Link *et al.*, J. Phys. Chem. B 2002, 106:3410-3415; Huang & Murray, J. Phys. Chem. B 2001, 105:12498-12502). Larger Au_n nanodots have also been produced with strong

luminescence throughout the visible region (Zheng, *et al.*, Phys. Rev. Lett 2004, 93: No. 077402).

[0138] Second and fourth generation OH-terminated PAMAM (G2-OH and G4-OH, respectively, Aldrich) were utilized to stabilize and solubilize gold nanoclusters in both aqueous and methanol solutions. By dissolving 0.5 μmol G4-OH or G2-OH and 1.5 μmol $HAuCl_4 \cdot nH_2O$ (Aldrich) into 2 mL of distilled water (18 MΩ), gold ions were sequestered into dendrimers and reduced by slowly adding an equivalent of $NaBH_4$ into the solution. Reduced gold atoms aggregated within the dendrimers to form small nanodots (dendrimer-encapsulated nanoclusters) and large nanoparticles. The solution was stirred for two days until reaction and aggregation processes were completed. Solutions were subsequently purified through centrifugation (13,000 – 23,000 g) to remove the large gold nanoparticles (Crooks *et al.*, Accounts Chem. Res. 2001, 34:181-190; Esumi *et al.*, Langmuir 1998, 14:3157-3159), leaving a clear, colorless, Au_8 nanodot solution. Although weak compared to the 285 nm pure dendrimer peak (see Fig. 5A), a clear absorption spectrum of dendrimer encapsulated gold nanoclusters was obtained by subtracting the pure dendrimer absorption. It can be seen from Fig. 5B that a new absorption band at 384 nm with bandwidth of ~60 nm (FWHM) appeared in the final fluorescent Au nanodot solutions. Contrary to the absorption spectrum of large gold nanoparticles, no surface plasmon absorption at 520 nm was observed from this solution, indicating that the nanodots are smaller than ~2 nm (Crooks *et al.*, Accounts Chem. Res. 2001, 34:181-190; Esumi *et al.*, Langmuir 1998, 14:3157-3159).

[0139] Strong blue luminescence with excitation and emission maxima at 384 nm and 450 nm, respectively, was clearly observed from these dendrimer encapsulated gold nanodot solutions (Fig. 6). The fluorescence excitation maximum and bandwidth were identical to the nanodot absorption band in Fig. 5B. While G2-OH and G4-OH dendrimers yielded indistinguishable fluorescent solutions, under the same synthetic conditions, G0 dendrimers yielded only non-fluorescent solutions with black gold solids. These heterogeneous solutions suggest that, unlike larger 2^{nd} and 4^{th} generation PAMAM, small 0^{th} generation dendrimers do not adequately protect and stabilize gold nanoclusters. Amazingly, for 384-nm excitation, integrated fluorescence quantum yields for G4-OH and G2-OH encapsulated gold nanodots were 41% ± 5% using similarly emitting quinine sulfate as the reference. The quantum yield further increased in methanol to 52% + 5%. The time dependence of the emission showed that there are two lifetime components (Fig. 7A), which are characteristic of gold nanodot emission (Link *et al.*, J. Phys. Chem. B 2002, 106:3410-3415). The short lifetime component was 7.5 ns, which was dominant (93%) in

the emission and likely arose from singlet transitions between low lying d orbitals and excited sp bands of gold nanodots. The long lifetime component (2.8 μs, 7%) may be due to a triplet-singlet intraband transition (Link *et al.*, J. Phys. Chem. B 2002, 106:3410-3415; Huang & Murray, J. Phys. Chem. B 2001, 105:12498-12502).

[0140] The well-defined dendrimer structure allowed analysis of encapsulated nanocluster sizes with electrospray ionization (ESI) mass spectrometry. As shown in Fig. 7B, Au_8 was the dominant Au-containing component in the fluorescent solutions and its abundance directly correlates with fluorescence intensity, independent of sample preparation. Depending on the reduction conditions, Au concentrations, and dendrimer generations, different Au-containing peaks can appear in the mass spectra. In all cases (>20 differently prepared samples), blue fluorescence intensity was only related to the abundance of the Au_8-containing species observed in the mass spectra. In accord with stable nanoclusters having 8 valence electrons (one from each Au atom; Lin *et al.*, Inorg. Chem. 1991, 30:91-95), this dominant nanocluster was confirmed to be in the overall neutral oxidation state as even 100-fold excess of highly reducing BH_4^- did not alter the nanodot fluorescence. Confirmed through expected shifts relative to the dendrimer parent peak upon dissolution in D_2O instead of H_2O, five molecules of water were also found to be associated with the hydrophilic PAMAM dendrimer-Au complex. While five waters appeared to be the favored number, smaller peaks corresponding to Au_8 with other numbers of water molecules ranging from one to six were also observed in the mass spectra of other similarly prepared samples. The peaks containing Au_8 were only observed in the fluorescent Au nanodot solutions and fluorescence intensities of differently prepared solutions were directly proportional to relative abundance of the Au_8 nanodot peaks alone. Additionally, Au nanodot preparations using both $HAuCl_4$ and $AuBr_3$ yielded indistinguishable fluorescent solutions with identical mass spectra. This indicated that the highly efficient blue emission resulted from Au_8 nanodots. Different color emission can be produced by adjusting relative Au:dendrimer concentrations to produce larger Au nanodots (Zheng, *et al.*, Phys. Rev. Lett 2004, 93: No. 077402).

[0141] Luminescence from gold nanodots arises from transitions between the conduction electrons, leading to "Multielecton artificial atom" behavior in these nanosized noble metal species. To date Au_5, Au_8 Au_{13}, Au_{23} and Au_{31} have all been produced with high quantum yield in aqueous solution, (Zheng *et al.*, Phys. Rev. Lett 2004, 93: No. 077402). As nanocluster size decreases, the spacings between discrete states in each band increases, leading to a blue shift in fluorescence relative to that from larger nanodots. The more than 100-fold fluorescence quantum yield enhancement over that of differently

prepared larger nanoclusters probably results from two factors. The lower density of states present in very small Au_8 nanoclusters minimizes internal non-radiative relaxation pathways. Additionally, the larger dendrimer cage better protects these nanoclusters/nanodots from quenchers in solution.

[0142] In conclusion, monodisperse Au_8 nanodots were synthesized and stabilized in dendrimer PAMAM aqueous solution. Au_8 nanodots show strong size specific emission, and its quantum yield was measured to be ~41% in aqueous solution. Other nanodot sizes have also been produced with similarly high quantum yields in aqueous solution (Zheng *et al.*, Phys. Rev. Lett 2004, 93: No. 077402) Practical applications of gold nanodots as a novel fluorophore become possible due to more than 100-fold enhancement in quantum yield and their size-tunable absorption and emission.

Example 4

Generation of dendrite-encapsulated copper nanoclusters

[0143] Second and fourth generation OH-terminated PAMAM (G2-OH and G4-OH, respectively, Aldrich) were utilized to stabilize and solubilize copper nanoclusters in both aqueous and methanol solutions. By dissolving 0.5 μmol G4-OH or G2-OH and 1.5 μmol copper sulfate into 2 mL of distilled water (18 MΩ), copper ions were sequestered into dendrimers and reduced by slowly adding an equivalent of $NaBH_4$ into the solution. Reduced copper atoms aggregated within the dendrimers to form small nanodots (dendrimer-encapsulated nanoclusters) and nanoparticles, leaving a clear, yellow, copper nanodot solution.

[0144] Strong blue luminescence with excitation and emission maxima at 392 nm and 470 nm, respectively, was clearly observed from these dendrimer encapsulated copper nanodot solutions (Fig. 8). The experiments are repeated with different generations of PAMAM dendrimers, and the emission and excitation spectra determined. The quantum yields are determined for the different generation dendrimer encapsulated copper nanoclusters. The dendrimer structure allows analysis of the encapsulated nanocluster sizes with electrospray ionization (ESI) mass spectrometry. Depending on the reduction conditions, copper concentrations, and dendrimer generations, different copper-containing peaks appear in the mass spectra. Further characterization of the dendrimer encapsulated copper nanoclusters is performed as described in Examples 5-6 for dendrimer encapsulated silver nanodots.

Example 5

Optimizing and controlling the generation of water-soluble, photoactivated, fluorescent Ag nanodots.

[0145] While dendrimers and chemical reducing agents are commonly employed for synthesis of large metal and semiconducting nanoparticles, much smaller Ag nanodots are readily synthesized simply by adding a 0.5 mM aqueous $AgNO_3$ solution to that of the desired PAMAM dendrimer in the proper molar ratios and adjusting to neutral pH. Generally, no chemical reductants are added, but similar results can be achieved by slowly adding small amounts of $NaBH_4$ to circumvent photoactivation. In solutions without any added chemical reductants, no visible absorption and no fluorescence is observed in these mixtures as long as they are kept in the dark. However, after photoactivation of the entire solution with an unfiltered 100W Hg lamp for 5 minutes, both visible absorption near 450 nm and strong fluorescence appeared. Much faster photoactivation occurred within small volumes when the solutions were irradiated with higher intensity through the microscope and/or when photoreductants such as 9 ethyl cabazole were added prior to irradiation.

[0146] While this nanodot synthetic process works very well, it produces a wide distribution of nanodots with fluorescence throughout the visible spectrum. In order to narrow the distribution of synthesized nanodots, spectral properties must be correlated with creation conditions. Certain nanocluster sizes are likely to be created preferentially under specific excitation and concentration conditions. For example, it was noted that total fluorescence intensity and overall emission color are strong functions of the dendrimer generation used: 0^{th} generation dendrimers formed primarily yellow and green highly fluorescent nanodots at low Ag:dendrimer ratios of 0.3:1, while 4^{th} generation PAMAM required a much higher Ag:dendrimer ratio of 3:1 and produced nanodots of all colors. The reaction conditions are optimized by adjusting both Ag:dendrimer ratios and total concentrations in the reactions with 0^{th} through 4^{th} or higher generation dendrimers. Working at ratios that only begin to produce fluorescence in each dendrimer generation, the concentration of the smallest emitting nanoclusters may preferentially be enhanced. Aliquots from each solution are irradiated with different wavelength ranges for differing amounts of time. These solutions are compared with those obtained through sub-stoichiometrically added $NaBH_4$ solutions to compare chemical and photoreduction processes. An aliquot of each sample solution is assayed by mass spectrometry using electrospray ionization and compared with the signal from a non-photoactivated solution.

Parallel analyses with fluorescence microscopy and ESI-MS identify the spectral signatures of the smallest nanoclusters.

[0147] This set of experiments can routinely elucidate the distribution of Ag nanocluster sizes within the nanodot samples. Because the nanodots contain only a few atoms, nanodot sizes will likely at least loosely follow Poisson statistics (statistics of small numbers) giving predictable populations of silver atoms per dendrimer. Poisson statistics, however, assume that no other interactions are present to further bias the counting statistics. Because different nanoclusters will be more or less stable under different conditions, tuning nanodot creation conditions will yield a modified Poisson distribution, making experimental verification of relative populations critical to identifying the properties of each size nanodot. Adjusting the concentrations will alter the relative populations tempered by the extent of reaction at a given concentration. The offset from Poisson statistics will be a direct measure of the relative equilibrium concentrations and any preferential stabilization of specific nanocluster sizes. Thus, routinely changing concentrations of Ag for a given amount of dendrimer and assaying the mixtures both before and after photoactivation by mass spectrometry and fluorescence microscopy will yield detailed information on the equilibrium constants governing nanodot formation. These experiments will determine the necessary Ag concentrations to preferentially produce the desired silver nanocluster size within the nanodots and the equilibrium constants for each PAMAM generation.

[0148] Additionally, the numbers of nanodots of a given color will be counted in the fluorescence microscope field of view using a color CCD camera and fluorescence spectrometer. Image simulation, fitting, and processing software has been written in IDL (Interactive Data Language, Research Systems, Inc.), an open shell programming environment that is ideal for image and mathematical processing. While measuring single molecule fluorescence spectra can be a tedious method of doing this, a representative sample of individual nanodots is probed with the spectrometer to determine the number of differently emitting particles present in a given sample. Once spectral purity and narrowness of individual nanodot emission is confirmed, individual features is counted with a color CCD camera. A single-chip CCD with a standard mosaic filter to produce color images uses 4 pixels (one detecting red, one for blue, and two for green) to generate one composite color pixel. Small, diffraction limited features do not cover enough pixels to yield an accurate color on single chip color CCDs. When detected by such a camera, any small change in sample position will

actually be registered as a color change in the emission due to detection by different numbers of red, blue and green pixels. Because of the small size of each feature, a 3-chip CCD will give accurate color information. Using a three-chip CCD, the emission color of each particle will be identified and user-written particle counting software will be employed to automatically count the numbers of each color nanodot. The distribution of fluorescent colors from individual nanodots will be directly correlated with the mass spectrum of each photoactivated or chemically reduced solution to assign the colors to specific nanocluster sizes within each type of nanodot solution. The spectrometer will characterize the spectral width of nanodot emission while the CCD only gives overall color, but with higher sensitivity and time resolution. Thus, the combination is important for accurately characterizing the individual nanodots and their distribution resulting from a given set of creation conditions.

Example 6

Optimizing the synthesis of specific Ag nanodot sizes

[0149] The known pH sensitivity of PAMAM dendrimers and Ag ions and atoms is used to control Ag nanocluster size and therefore control spectral properties. PAMAM is well-known to increase in size with decreasing pH (Kleinman *et al.*, J. Phys. Chem. B 2000, 104:11472-11479; Lee *et al.*, Macromolecules 2002 35:4510-4520; and Bosman *et al.*, Chem. Rev. 1999 99:1665-1688). This size change makes the dendrimer exterior significantly more permeable and creates larger cavities to accommodate nanoclusters or even nanoparticles in their interiors. At high pH, the dendrimer is quite compact, thereby preventing ions from reaching the dendrimer core. This size behavior nicely complements the preference of silver for more basic environments. As a result, Ag ions and metal nanoclusters interact strongly with the basic amines on the dendrimer interior. As the pH decreases, the partitioning of Ag to the dendrimer interior should increase significantly. The increased dendrimer permeability and preference of Ag to interact with the dendrimer interior at acidic pH both suggest that larger nanoclusters are more readily formed at low pH. Since pH has a more significant effect on higher dendrimer generations, the pH studies will be performed with 4^{th} generation G4-OH and G4-NH_2 PAMAM dendrimers. This scheme is used to preferentially shift nanodot size distributions to larger and smaller sizes. As a function of pH, bulk absorption and emission spectra are measured, and individual

nanodots of a given color as described above are counted. Nanodot distribution is assayed as a function of both dendrimer generation and pH in order to gain control over nanodot spectral properties. Once the nanodots are created, pH will be returned to pH7 to assay stability of formed nanodots within the PAMAM host. ESI-MS is performed on all such solutions to directly correlate changes in optical properties with changes in Ag nanocluster sizes within the nanodot samples. Together, these methods allow determination of the spectral properties associated with specific Ag nanocluster sizes within the PAMAM dendrimers.

Photophysical characterization of dendrimer-encapsulated nanodots.

[0150] Bulk lifetime measurements are performed on the nanodots in the time domain utilizing a frequency doubled titanium sapphire laser for excitation at 400 nm (82MHz repetition rate, 200 fs pulse width), a fast photomultiplier tube and a time correlated single photon counting electronics. With deconvolution of instrument response, the primary fluorescence lifetime component of the Ag nanodots was determined to be ~30 ps. (Peyser-Capadona *et al.*, Phys. Rev. Lett. 2005, 94: 058301). Thus, the faster detection system is employed for facile measurement of sub-100 ps lifetimes on the bright emission from groups of Ag nanodots.

[0151] Absorption cross section measurements are made through comparison with single $DiIC_{18}$ molecules, a dye with a very well-characterized absorption cross section and one that has been worked with on the single molecule level (Bartko, & Dickson, J. Phys. Chem. B 1999, 103:3053-3056; Bartko & Dickson, J. Phys. Chem. B 1999, 103:11237-11241; and Bartko *et al.*, Chem. Phys. Lett. 2002, 358:459-465). Confirming single molecule behavior through identifying blinking species and those simultaneously exhibiting dipole emission patterns allows for the circumvention of not knowing the exact concentration within a given sample, and simply measuring the strength of absorption relative to a single molecule of known absorption cross section and comparing the saturation intensities. Using the combination of individual nanodot spectra, their distributions within a given nanodot solution, and their corresponding absorption cross sections, the concentrations of each nanodot species is determined within a given sample. This will be useful in determining the optical density of a given color nanodot within a given solution and by using the initial concentrations of dendrimer and silver, the equilibrium constants for nanodot formation are determined.

[0152] Using the measured concentrations of each size nanodot and its contribution to the total solution absorption, the optical density of a given nanodot type

is determined. Through comparisons with methanolic rhodamine 6G solutions, nanodot solutions of the same optical density are prepared. Fluorescence quantum yields are measured through exciting at a wavelength with nanodot optical density identical to that of one of the standard rhodamine solutions. The ratio of rhodamine fluorescence intensity to that of the desired nanocluster when looking within its characteristic spectral window (after accounting for the much smaller, but measured contributions from the other nanoclusters in solution) will directly yield the quantum yield of each nanodot. This ratiometric method allows accurate quantum yield measurements without having to know the absolute nanodot concentration because the number of photons absorbed is the same for both the rhodamine 6G reference and the nanodot being probed. Together, the mass spectrometry and photophysical characterizations of both bulk and single molecule samples will definitively determine the sizes and photophysical signatures of each color of nanodots. This information will also lead to improved synthetic methodologies for preferentially enriching one nanodot size over others.

Fluorescence stability

[0153] Largely unaffected by environmental interactions, the dendrimer-stabilized emission is further explored to yield quantitatively similar emission for a given nanodot in a wide variety of different environs. Such environmental insensitivity is in stark contrast to that of II-VI (e.g. CdSe) quantum dots in which surface passivation is crucial to overall photophysical properties due to the presence of trap states on the surface (Bruchez *et al.*, Science 1998, 281:2013-2016; Chan & Nie, Science 1998 281:2016-2018; Nirmal *et al.*, Nature 1996 383:802-804; Huynh *et al.*, Adv. Mater. 1999 11:923; Alivisatos, Endeavour 1997, 21:56-60; Klimov *et al.*, Phys. Rev. B 2000, 61:R13349-R13352). The dendrimer-encapsulated nanodots appear to circumvent such difficulties by having the chromophore ensconced within the water-soluble dendrimer core. The blinking (fluorescence intermittency) is probed as a function of ionic strength and pH. Commonly used buffers such as phosphate buffers and sodium acetate/acetic acid are used to simultaneously control pH while adjusting ionic strength. Quenchers ranging from acrylamide to dyes with different absorptions are added to each nanodot solution to assay for energy transfer from the Ag nanodot. Stern-Volmer quenching studies are performed to determine the extent of quenching and, therefore, the influence of the dendrimer on the nanocluster stabilization and isolation from the environment. The fast lifetimes, however, suggest that these

nanodots will be largely insensitive to quenching. In addition to blinking and total emission intensity, the fluorescence lifetime and spectra will also be measured to assay whether any changes occur due to environmental interactions. With their very strong transitions and short lifetimes, however, they are likely to make excellent acceptors in FRET donor-acceptor pairs. Both bulk and single molecule experiments decipher if any change in photophysical dynamics results from altered blinking dynamics or an average overall reduction in fluorescence efficiency. The host density and size of the dendrimers is also adjusted. Ag nanodot blinking dynamics and photophysical parameters in 0^{th} through 4^{th} generation PAMAM dendrimers are probed to directly determine the protection afforded by successively larger and higher density dendrimer hosts. These studies will directly assay the extent of penetration of solvent and quenchers into the dendrimer core.

Orientational Dynamics

[0154] The orientational dynamics of linearly polarized individual surface bound nanodots are investigated for two reasons: geometry changes of small Ag nanoclusters are thought to result in very different absorption and emission wavelengths (Harbich *et al.*, J. Chem. Phys. 1990, 93:8535-8543; Fedrigo *et al.*, J. Chem. Phys. 1993, 99:5712-5717; Rabin *et al.*, Chem. Phys. Lett. 2000, 320:59-64) and the orientational information may be very useful in biological labeling experiments, whether used for energy transfer measurements or following the orientational motion of individual proteins. This is in contrast to the much larger CdSe quantum dots, which are not linearly polarized, but instead emit in all directions, being characterized by a unique "dark" axis (Empedocles *et al.*, Nature 1999, 399:126-130). Thus, correlating orientational dynamics of the nanocluster with any observed spectral changes will be very important to understanding if geometry changes also give rise to differently colored Ag nanodots. These experiments will also be performed with the 3-chip color CCD to obtain color emission patterns. In order to confirm that the spectrum is indeed narrow single nanodot fluorescence spectra will be taken through the microscope coupled spectrograph using a 150 l/mm diffraction grating. The orientational trajectories are fit to the models of dipolar emission at an interface (Bartko *et al.*, J. Phys. Chem. B 1999,103:3053-3056; Bartko & Dickson, J. Phys. Chem. B 1999, 103:11237-11241; Hollars & Dunn, J. Chem. Phys. 2000, 112:7822-7830; Hellen & Axelrod, J. Opt. Soc. Am. B-Opt. Phys. 1987, 4:337-350) as viewed

through an optical microscope to follow true 3-D nanocluster orientational dynamics resulting from any nanocluster mobility within the dendrimer hosts.

Example 7

Peptide encapsulation of silver nanodots

[0155] Attempting to utilize the vast diversity inherent in biological systems (Whaley *et al.*, Nature 2000, 405:665-668; Lee *et al.*, Science 2002, 296, 892-5; and Seeman & Belcher, 2002 Proc. Nat. Acad. Sci., USA, 99 Suppl 2:6451-5), it was demonstrated that a short 9-amino acid peptide can stabilize Ag_n nanocluster fluorescence. A short peptide having the sequence AHHAHHAAD (SEQ ID NO:1) was recently reported to interact with large metal and semiconductor nanoparticles upon $NaBH_4$ reduction (Djalali *et al.*, J. Am. Chem. Soc. 2002 124:13660-13661; Slocik *et al.*, Nano Lett. 2002 2:169-173). Using the gentle photoactivation procedures described herein, very highly fluorescent peptide-encapsulated nanodots at Ag:peptide molar ratios of 0.1:1 were produced without chemical reducing agents, but can also be produced through the use of photoreductants and UV/blue laser or lamp illumination. Using this peptide, fluorescence images were devoid of nearly all red and orange emitters, indicating a narrower fluorescence distribution than those nanodots stabilized by the larger dendrimers. Thus, the stronger and more specific binding of even this first attempt at peptide encapsulation preferentially creates shorter wavelength-emitting (and presumably smaller) Ag nanoclusters within the peptide scaffold with a narrower size distribution. This result strongly bolsters the hypotheses that highly selective nanodot-binding peptides can be identified through the proposed screening methods, and that different peptides are likely to stabilize nanodots of different sizes/colors. These same species exhibited strong single molecule Raman spectra of the peptide, as enhanced by the Ag nanocluster (see below and Peyser-Capadona. *et al.*, Phys. Rev. Lett. 2005, 94: 058301)

[0156] Extremely small, highly fluorescent and incredibly photostable, water-soluble Ag nanodots were produced consisting of only a few atoms encapsulated by both PAMAM dendrimers and short peptides. The extremely advantageous optical properties have yielded incredibly photostable and strongly absorbing and emitting species with size-dependent emission throughout the visible region. One can utilize single molecule microscopies and water-soluble noble metal nanoclusters to create and

characterize even more powerful labeling methods and materials. These specific, multicolored labels allow for single molecule experiments with high sensitivity, greatly enhanced ease, and experimental simplicity. New fluorescent and Raman probe developments of this type are crucial to the general applicability and utility of single molecule methods in unraveling the complexities of biological systems.

Example 8

Identification of optimal peptides for encapsulation of silver nanodots

[0157] Because Ag is biocompatible and can be non-toxic, it provides unique opportunities for simultaneously developing the smallest and brightest possible *in vivo* fluorescent biolabels. These same methods can be applied to gold and copper nanodot formation within peptide scaffolds. Dendrimer-encapsulated nanodots can already be employed as small, extremely bright biocompatible labels. Although much smaller than GFP, the 3.272 kD 2nd generation PAMAM dendrimer is still larger than most organic dyes. To further explore the potential of using Ag nanodots as biological labels, specific peptide sequences are identified that can specifically bind to differently sized metal nanoclusters and their true prospects for specific multicolor labeling of biomolecules are assessed. By creating and searching peptide libraries for Ag nanodot fluorescence, the most tightly binding sequences are identified. Nanodots formed within these sequences are assayed for stability, photoactivation, and photophysical properties. The relative stability will also be assessed relative to the dendrimer hosts. In this manner, transfer of the nanocluster is investigated between the dendrimer and the peptides.

Experimental approach

[0158] Many protein-ligand interaction studies make use of the phage display technique for identifying peptides that bind to other molecules (Wolcke & Weinhold, Nucleosides Nucleotides Nucleic Acids 2001, 20:1239-41; Krook *et al.*, Biochem Biophys Res Commun 1994, 204:849-54; Nicholls *et al.*, J. Molecular Recognition 1996, 9:652-7 (1996); Stern & Gershoni, Methods Mol. Biol. 1998, 87, 137-54). Although a powerful approach, phage display requires one of the interaction components to be immobilized on solid surfaces. Application of phage-based peptide library screening has also recently been demonstrated in the synthesis and stabilization of unique inorganic materials (Whaley *et al.*, Nature 2000, 405:665-668; Lee *et al.*,

Science 2002, 296:892-895; Seeman & Belcher, Proc. Natl. Acad. Sci. USA 2002, 99:6451-6455). Because the target peptides will stabilize strong Ag nanocluster fluorescence in solution, Ag_n-binding peptides are identified with an *E. coli* based system (FliTrx random peptide display library, Invitrogen) coupled with fluorescence-activated cell sorting (FACS). The combination of the two techniques will allow a solution based screening strategy. The FliTrx peptide library displays peptides on the surface of *E. coli* using the major bacterial flagellar protein (FliC) and thioredoxin (TrxA). The commercially available FliTrx library is composed of a diverse set of random dodecapeptides inserted into the active site loop of thioredoxin, which is itself inserted into the dispensable region of the flagellin. The random dodecapeptides are constrained by a disulfide bond formed within TrxA. Adding tryptophan to the culture can induce the expression of peptide protein fusion, and this will ensure that all peptide fusions are displayed at the same time. When induced, the fusion protein is exported and assembled into flagella on the bacterial cell surface, allowing display of the constrained peptide. As these peptides are produced on the outside of the *E. coli* cell in high copy numbers, it is these peptides that will be assayed for stabilization of Ag nanodot fluorescence. The population of bacteria is then sorted according to the fluorescence properties with flow cytometry to isolate those bacteria emitting fluorescence.

Optimization of Ag_n nanodot production on displayed FliTrx peptides

[0159] Optimal photoreduction conditions for peptide encapsulated nanodot formation on the bacterial surface are determined through optical microscopy using the previously identified Ag_n (see Example 7). An oligonucleotide encoding the nonopeptide sequence and flanking *Bgl*II and *Eco*RV recognition sequences is synthesized (Operon Co.) and cloned into the multicloning sites of the pFliTrx vector obtained from Invitrogen Co. This construct will insert the peptide into the nonessential region of flagellin as described above. The plasmid is isolated and transformed into the host strain GI826 (Invitrogen) resulting in the display of the peptide on the surface of *E. coli*. This strain is then used to identify photoactivation and chemical reduction conditions suitable for creating fluorescent peptide-encapsulated Ag nanodots when screening the FliTrx libraries with FACS. Cell viability is assessed when illuminated with blue light and when exposed to BH_4^- reduction as well as the efficiency of generating Ag nanodots. Initially, the total fluorescence from individual bacteria will be measured as a function of photoreduction

time for many different Ag^+ concentrations through optical microscopy. This procedure is quite straightforward and consists of photochemically reducing Ag ions with electron donors in solution (Tani & Murofushi, J. Imag. Sci. Technol. 1994, 98:1-9; Stellacci *et al.*, Adv. Mater. 2002, 14:194; Eachus *et al.*, Annu. Rev. Phys. Chem. 1999, 50:117-144). This procedure works well due to the advantageous energy levels of Ag relative to those of electronically excited molecules (Tani & Murofushi, J. Imag. Sci. Technol. 1994, 98:1-9; Marchetti *et al.*, J. Phys. Chem. B 1998, 102:5287-5297; Stellacci *et al.*, Adv. Mater. 2002, 14:194; Eachus *et al.*, Annu. Rev. Phys. Chem. 1999, 50:117-144). Photoreduction coupled with added photoreductants provides the opportunity to control the nanocluster size and color due to the different reduction potentials for Ag nanoclusters composed of only a few atoms (i.e. Ag_{2-8}). Alternatively, chemical reduction can be employed by slowly adding up to an equivalent of $NaBH_4$ or other reducing agents, thereby also yielding fluorescent nanodots. The conditions producing the most highly fluorescent Ag nanodot labeled *E. coli* cells will be the initial conditions for all library searching studies. Using the strong fluorescence producing conditions identified, the fluorescent bacterial culture will be washed and subsequently suspended in phosphate buffer for FACS analysis. This washed suspension of *E. coli* will also be re-assayed for total fluorescence on the microscope stage to assess the stability of fluorescence residing on the bacterial surface during the process of sample preparation.

Identification of specific Ag nanodot binding sequence through random peptide display libraries

[0160] A commercial display library (Invitrogen) will initially be used that contains a diversity of $1.8x10^8$ to identify peptide sequences that interact specifically with Ag nanoclusters. Prepared libraries will be separated into 50 vials and frozen for individual analysis and optimization of Ag nanodot binding conditions as determined by total fluorescence. Each vial will contain most of the peptide library and will be assayed for optimal Ag_n binding conditions through a low magnification objective on the optical microscope stage. First, the library culture will be grown in the presence of tryptophan for 6 hours to induce the expression of fusion flagellins. The culture will be washed with phosphate buffer and then incubated with silver nitrate to form Ag nanodots by photoreduction.

[0161] Flow cytometry is capable of correlating cell/particle size with fluorescence. A dot plot of FSC (forward scatter, to define relative size) and SSC (side-

scatter, to define relative granularity) will be generated (CellQuest program) to define a gate that specifies the bacterial population for sorting using FACS. The bacteria will be sorted according to the overall fluorescence intensity distribution. Three fluorescence detecting channels are available: FL1, 530 nm with a 30 nm width, FL2, 585 nm with a 42 nm width, and FL3, 650 nm and above, each or combinations of which can be utilized for cell sorting. It is expected the majority of the bacteria with Ag nanocluster non-binding peptides will have minimal fluorescence and only those with significant fluorescence will be recovered. However, the intensity of fluorescence in each channel will be used in conjunction with the forward scatter to identify highly fluorescent cells resulting from Ag_n binding and stabilization. The collected bacteria will be plated out on ampicillin selection agar plates to isolate single colonies. Each single colony will be saved and tested again with flow cytometry and optical microscopy to confirm the associated fluorescence phenotype. Once the intensity of fluorescence is determined, plasmid DNA will be isolated from those bacteria with bright nanodot fluorescence and the peptide sequence determined by direct sequencing analysis. Alignment of sequences from the positive clones may generate a contiguous consensus peptide sequence; alternatively, a structural motif formed by discontinuous conserved residues may be recognized. The defined sequences will be synthesized by solid phase peptide synthesis, and its binding properties to the Ag nanodots characterized using fluorescence microscopy, photophysical characterizations and mass spectrometry, similar to the studies discussed above.

Creating user-defined libraries into FliTrx peptide display system

[0162] An alternative to the use of a commercial library screen, flagellin display libraries can be generated with different peptide lengths using the pFliTrx vector. Degenerate oligonucleotides of 15 bp (5 a.a.), 27 bp (9 a.a.), 45 bp (15 a.a.), and 60 bp (20 a.a.) flanked by *Bgl*II and *Eco*RV restriction recognition sequences will be synthesized (Operon Co.). The mixtures of oligonucleotides will be digested with these two enzymes and cloned into the pFliTrx vector, which has been cut with the same enzymes. The plasmid isolated from the collection of clones will then be transformed into the test strain GI826, and the screening procedures repeated as described above.

[0163] This method utilizes the natural diversity of the amino acids to select for specific Ag nanocluster binding to form a biocompatible, highly fluorescent nanodot. In many ways this is similar to the common method of genetically attaching a $(His)_6$-

tag on the N- or C- terminus of a protein of interest to be purified through specific interaction with Ni. Analogously, the identified Ag_n-binding peptides defined in this study will specifically and selectively bind Ag nanoclusters, thereby enhancing their fluorescence. Additionally, the multiple fluorescence detection channels in FACS will also allow identification of a suite of peptides that preferentially stabilize different size, and therefore color, nanodots.

Characterization of Ag_n nanocluster-binding peptides

[0164] Once optimal peptide lengths and sequences are routinely identified and synthesized, environmental stabilities and photophysical properties of the fluorescent nanoclusters are directly assayed as described for the dendrimer-encapsulated nanodots above. While it is likely that specific sequences will preferentially stabilize specific nanocluster sizes with much narrower emission than possible in PAMAM dendrimer hosts, the same particle counting methods to identify the numbers of each type of nanocluster encapsulated within each flavor of peptide will be characterized. In fact, even in the preliminary peptide used that allows and stabilizes Ag nanodot fluorescence, a narrowing of the nanodot size distribution is seen relative to that upon dendrimer encapsulation. Because of the affinity of Ag_n for more basic residues, larger nanoclusters will likely be preferentially stabilized by more basic sequences. This is likely to impart size and therefore nanodot selectivity in peptide-Ag binding interactions. Consequently, this genetic selection of Ag nanodot binding peptides is likely to result in a variety of peptides, each of which stabilize different nanoclusters. This will result in a range of different programmable labels with different optical properties, each of which can be used as an independent single biomolecule label. Mass spectrometry (ESI and MALDI) will be performed on all peptides that are synthesized and subsequently tested for Ag_n nanodot binding in order to determine the nanocluster size distribution within each identified Ag_n-binding peptide and its correlation with the number of emitters of a given color. This correlated single nanodot fluorescence microscopy, bulk absorption and emission, and mass spectrometry analysis for differing peptide and silver ion concentrations will directly characterize the binding constants for each peptide identified through FACS library screening.

Example 9

Transfer of Ag nanoclusters between dendrimers and peptides

[0165] Because silver salts generally have very limited solubility in water, AgCl will likely precipitate out of a biologically relevant solution due to its very small solubility product and the large amount of chloride ions present in biological media. This presents a potential problem for delivering Ag_n nanoclusters to the peptides defined in the studies proposed above, and may limit the direct delivery of highly fluorescent Ag nanoclusters. However, Ag nanoclusters were found to be very stable when encapsulated in the dendrimer hosts and retain their very bright fluorescence at physiological NaCl concentrations. Even the small 2nd generation PAMAM dendrimer effectively shields the Ag nanoclusters from AgCl precipitation. In addition, dendrimers are well known to readily transport material contained within their interior across biological membranes (Toth *et al.*, STP Pharma Sci. 1999, 9:93-99; Bielinska *et al.*, Biomaterials 2000, 21:877-887; Luo *et al.*, Macromolecules 2002, 35:3456-3462; Yoo *et al.*, Pharm. Res. 1999, 16,:1799-1804; Wiwattanapatapee *et al.*, Pharm. Res. 2000, 17:991-998; Esfand, & Tomalia, Drug Discov. Today 2001, 6:427-436), a valuable property in developing *in vivo* labeling experiments. As a result, the small PAMAM dendrimers are investigated as vehicles to transfer the Ag nanoclusters directly to the identified peptides that strongly bind Ag nanoclusters. Ag nanodot transfer is investigated with the same screening methods as peptide identification and selection. Instead of optimizing silver ion concentrations for effective labeling of peptides within the FliTrx libraries, the dendrimer-encapsulated nanodot concentrations is adjusted while viewing solutions on the microscope stage (with a 10x objective) to monitor nanodot exchange. Once conditions that label the *E. coli* cells are identified, peptide libraries are specifically screened for those cells containing peptides capable of acquiring the nanodots from the dendrimers. Because flow cytometry can select cells based on scatter and fluorescence, the very small dendrimers are undetectable in both channels. Only the cells are sufficiently large to scatter enough light to initiate collection, thereby avoiding false positives due to dendrimer-encapsulated nanodot fluorescence. Additionally, each bacterium within the FliTrx library has thousands of peptide copies, thus providing the potential for much stronger fluorescence signals. Only those cells exhibiting strong fluorescence and scattered light are collected, grown

with ampicillin selection, and sequenced. Such dendrimer to peptide library nanodot transfer is likely to be favored for lower generation PAMAM dendrimers under specific environmental conditions, such as specific pH's at which the dendrimer-encapsulated nanodots can more easily escape. The most pH-stable peptide-encapsulated nanodots are therefore likely to be of great utility in future labeling experiments. This additional screening method will further select for peptides that will preferentially extract Ag nanoclusters from the dendrimer, opening possibilities for facile labeling of proteins both *in vitro* and *in vivo*.

Example 10

Generation and characterization of oligonucleotide encapsulated nanoclusters

[0166] The high affinity of Ag+ for DNA bases has allowed the creation of short oligonucleotide-encapsulated Ag nanoclusters without formation of large nanoparticles. Experimental approach

[0167] Silver nitrate (Aldrich, 99.998%) and sodium borohydride (Fisher, 98%) were used as received. Oligonucleotides (Integrated DNA Technologies) were purified by desalting by the manufacturer. The 12-base single-stranded oligonucleotide 5'-AGGTCGCCGCCC-3' (SEQ ID NO:2) was received as dehydrated pellets and dissolved in a 5 mM phosphate buffer (pH = 7.5). This oligonucleotide sequence was used as it favors the single-stranded vs. hairpin or self-dimer forms. Reactions were conducted in either 5 mM phosphate or 100 mM $NaClO_4$/5 mM phosphate buffer (Norden *et al.*, 1996, Biopolymers, 25:1531-1545), containing 60 μM silver nitrate, 60 μM sodium borohydride, and 10 μM of SEQ ID NO:2. Alternatively, 10 μM of any of SEQ ID NOs:3-8 were used. The silver nanoclusters were synthesized by first cooling the solution of DNA and Ag+ to 0°C and then adding $NaBH_4$ followed by vigorous shaking.

[0168] Visible absorption spectra were acquired using a Shimadzu UV-2101PC spectrometer. Circular dichroism spectra were obtained from a Jasco J-710 spectropolarimeter. Fluorescence spectra were acquired on a Shimadzu RF-5301PC spectrofluorimeter. Mass spectra were acquired using a Micromass Quattro LC operated in negative ion mode with 2.5 kV needle and 40 V cone voltages. NMR spectra were acquired on a Bruker DRX 500 operating at 500 MHz.

Results

Base Association

[0169] Ag^+ strongly favored association with the heterocyclic bases and not the phosphates (Eichhorn, In Inorganic Biochemistry; Eichhorn, G. L., Ed.; Elsevier: New York, 1973; Vol. 2, Chapter 33; Marzilli, In Progress in Inorganic Chemistry; Lippard, S. J., Ed.; John Wiley and Sons: New York, 1977, Vol. 23, pp. 255-378). For Ag^+:base concentrations less than 0.2, complexes formed with the purines via nitrogen or π-electron coordination. For higher silver concentrations ($0.2 < Ag^+$:base < 0.5), a weaker complex formed and involved coordination with the nitrogens of either the purines or pyrimidines. Changes were found in the electronic absorption and circular dichroism spectra that indicated the silver ions and nanoclusters associated with the bases. For the 12-base oligonucleotide, the DNA absorption maximum (λ_{max}) shifted from 257 nm to 267 nm upon Ag^+ complexation (1 Ag^+:2 bases) (Fig. 9). Following reduction of the bound ions, further spectral changes occurred. Initially, λ_{max} shifted from 267 nm to 256 nm, and the molar absorptivity increased. This latter effect may be attributed to new, overlapping electronic bands for small silver clusters, which are known to absorb in this spectral region (Harbich *et al.*, 1990 J. Chem. Phys., 93, 8535-8543). Alternatively, the dipole coupling between the excited electronic states of the bases could have been altered by structural changes induced by the silver nanoclusters, a possibility also suggested by the circular dichroism (CD) spectra. Eventually, as Ag nanoclusters grew and visible absorptions evolved, the λ_{max} shifted to 262 nm and the molar absorptivity decreased.

[0170] The electronic transition of the bases exhibited a small CD due to the chirality of the riboses, and this spectroscopic technique is sensitive to the arrangement of the bases (Rodger & Norden, Circular Dichroism and Linear Dichroism, Oxford, New York, 1997). For the Ag^+ complex with double-stranded DNA, circular and linear dichroism studies showed that Ag^+ induced nonplanar and tilted orientations of the bases relative to the helical axis (Norden *et al.*, 1996, Biopolymers, 25:1531-1545). For the single-stranded oligonucleotide, the CD spectra was similar to that for double-stranded DNA, suggesting that Ag^+ may cause similar perturbation of the bases in single-stranded DNA (Fig. 10). Analogous to the evolution of the absorption spectra (Fig. 9), the CD spectra also changed upon reduction of the Ag^+. The differences between the spectra in Fig. 10 indicate that the silver nanoclusters induced different structural changes in DNA than does Ag^+.

Nanocluster Sizes

[0171] Because of the monodispersity of synthesized DNA oligonucleotides, the stoichiometry of the nanoclusters can be accurately determined using electrospray mass spectrometry (Fig. 11). These experiments were conducted in water to reduce the concentrations of cations that would form adducts with the DNA and consequently reduce sensitivity. The experiments also used a higher concentration of oligonucleotide (75 μM) to enhance the ion abundance. In Fig. 11A, the dominant peak in the spectrum occurs at 3607 amu, as expected for the 12 base oligonucleotide. Addition of 6 Ag^+:oligonucleotide (1 Ag^+:2 bases) resulted in complexes with a maximum of 4 Ag^+ per DNA strand. This difference between the total and bound ion concentrations may be attributed to the weaker adducts that form at higher silver concentrations (Yamane & Davidson, 1962 Biochim. Biophys. Acta, 55, 609-621), which may be more susceptible to dissociation during desolvation and/or ionization. A poor description of the ion intensities was observed when they were fit as a Poisson distribution, which suggested that 4 Ag^+/oligonucleotide was the favored stoichiometry (Fig. 11A). The DNA sequence used for these studies favored the single-stranded form as opposed to self-duplex or hairpin forms. The mass spectra indicated that the clusters are also bound to a single DNA strand. Following reduction of the bound Ag^+ ions, the number of bound silver atoms was initially small, but the distribution shifted to higher stoichiometries with time (Fig. 11B-D). As opposed to the Ag^+ complexes, a Poisson distribution gave a more accurate description of the ion distributions for the reduced complexes. The following average cluster sizes were measured: 1.8 ± 0.3 (50 minutes), 2.4 ± 0.2 (350 minutes), and 3.0 ± 0.2 (1050 minutes). The observed distribution terminated at 4 Ag/oligonucleotide, which again differs from a Poisson distribution. End effects may contribute to the stoichiometries of both the ion and metal complexes with these short oligonucleotides, but spectroscopic studies directly suggested that the base sequence was a significant feature of the interaction of the nanoclusters with DNA. Single clusters or multiple smaller clusters may be bound to a single oligonucleotide.

Nanocluster Spectra

[0172] Mass spectrometry demonstrated that a small number (≤ 4) of silver atoms are bound to the single-stranded DNA template, and the following spectroscopic studies demonstrated that these silver atoms form nanoclusters. Reduction of the Ag^+

bound to the DNA resulted in new species with electronic transitions in the visible region of the spectrum (Fig. 12). The transition that was most prominent initially had a λ_{max} = 426 nm at 9 minutes after adding the BH_4^-. Over a period of 12 hours, the absorbance of this band decreased and a broad absorption band with peaks at 424 and 520 nm developed. As determined through theoretical and low temperature spectroscopic studies, electronic transitions for small silver clusters, in particular Ag_2 and Ag_3, are expected in this spectral region Harbich *et al.*, 1990 *J. Chem. Phys.*, 93, 8535-8543; Bonacic-Koutecky *et al.*, 1999 *J. Chem. Phys.*, 110, 3876-3886; Marchetti *et al.*, 1998 *J. Phys. Chem. B*, 102, 5287-5297). Using these prior studies, a definitive assignment of the electronic bands was problematic because the peaks for the DNA-bound cluster were expected to shift and broaden relative to their gas-phase and rare gas matrix-isolated values. No change in the absorbances or peak positions was observed when the solutions were centrifuged, indicating that the spectra cannot be attributed to nanoparticles. Similar spectra were observed when 2 BH_4^-:1 Ag^+ wais used, indicating that the spectra arose from fully reduced silver clusters (not shown). In a buffer with 100 mM $NaClO_4$, the results were similar to those in the lower salt buffer, with the only difference being a broad band without distinct peaks after longer times. This similarity suggested nanocluster formation was not impeded by competing cations, which is consistent with their association via the bases and not the phosphates.

[0173] Because the small silver clusters did not have inherent chirality, the induced CD associated with the Ag nanocluster electronic transitions was further evidence that the clusters were bound to the DNA (Fig. 13). The most prominent band had a minimum response at 440 nm and this minimum shifted to longer wavelengths with time. However, unlike the absorption spectra, the magnitude of this response did not diminish with time. A shoulder at 500 nm suggested the species that contributed to the longer wavelength absorptions (Fig. 12) were also bound to the DNA strand.

[0174] As opposed to larger metal nanoparticles, a distinctive feature of small nanoclusters is their strong fluorescence due to their lower density of electronic states. For the DNA bound nanoclusters, prominent fluorescence was observed at ≈ 630 nm (Fig. 14A-B). For excitation between 240 and 300 nm, a band at 630 nm was observed with the maximum intensity observed using 260 nm excitation. While this result suggested the cluster emission occurred via energy transfer, the silver clusters also had

higher lying excited states accessible in this spectral region. Thus, emission following direct excitation of the higher electronic bands of the silver clusters is also feasible.

[0175] The multiple peaks in the absorption and circular dichroism spectra suggested the presence of small clusters with varying stoichiometries. The fluorescence spectra provided further evidence that the samples contained multiple species, but the mass spectra indicated that each DNA strand encapsulates only a single Ag nanocluster. First, the maximum emission intensity (λ_{max} = 638 nm) occurred with an excitation wavelength of 560 nm (Fig. 14A-B), which is significantly red-shifted relative to the absorption maximum at 520 (Fig. 12). Second, for excitation at wavelengths greater than 500 nm, the wavelength of maximum emission shifted to longer wavelengths as the excitation wavelength increased. One possibility suggested by Fig. 14A-B is that the emission band for the 560 nm excitation can be spectrally decomposed as the emission bands for 540 and 580 nm excitation. In other words, at least two distinct species contributed to the fluorescence in this wavelength region.

[0176] As suggested by the absorption spectra, NMR spectra also indicated that the silver nanoclusters interacted directly with the DNA bases. The aromatic proton resonances in the ^{1}H NMR spectra of the oligonucleotide were well resolved prior to the addition of Ag^+ (Fig 15). However, the proton resonances were essentially broadened to baseline upon addition of Ag^+ (spectrum not shown). In contrast, most of the aromatic proton resonances in the ^{1}H spectra with silver clusters were almost as narrow as those of the free oligonucleotide (Fig. 15). The cytosine H6 proton resonances exhibited the largest change in chemical shift in the presence of the silver nanoclusters (Fig. 15). Similar upfield chemical shift changes were also observed for the H5 protons of cytosine (spectrum not shown). These observations indicate that the cytosine bases are most favored for interaction with the silver nanoclusters. The six cytosine H6 resonances were identified in 1D spectra based upon their splitting due to H6-H5 coupling, and by H6-H5 crosspeaks in 2D COSY spectra. However, it was not possible to determine the sequence position of each cystosine resonance in the proton spectrum. Nevertheless, the different chemical shift changes exhibited by the cytosine H6 resonances indicated that cytosine bases interact with silver clusters in a sequence-dependent manner.

Concentration Studies

[0177] To investigate the importance of the relative Ag^+:DNA stoichiometry, a 10 μM concentration of each oligonucleotide was maintained while the Ag^+ concentration was reduced from 1 Ag^+:2 bases (Fig. 12) to 1 Ag^+:10 bases (Fig. 16A-B) and the cell path-length was increased five-fold. While the two sets of spectra were similar with respect to the overall absorbances and the wavelengths of the transitions, differences were observed. The maximum absorbance for the 420 nm peak occurred at 20 min for the more dilute sample, or about twice as long as for the more concentrated sample (Fig. 12). This slower rate is expected when intermolecular exchange results in the formation of specific and favored cluster stoichiometries. The width of the 440 nm band was much narrower in the more dilute sample as opposed to the more concentrated sample, which suggested that a range of binding sites with slightly different electronic effects were available for binding by the silver clusters. At the lower concentration, the more favored sites were occupied, leading to an overall narrowing of the spectral transition. Another difference was the presence of a new band at 360 nm, which was not associated with any fluorescence. No differences were observed in the fluorescence spectra of the concentrated and dilute samples. As such, it is feasible to control the formation of nanoclusters with specific stoichiometries using DNA strands with specific sequences. To date, different silver nanocluster sizes and emission colors in various ss-DNA and ds-DNA lengths and sequences have been created (including C_{12} (SEQ ID NO:3), C_{24} (SEQ ID NO:4), C_{36} (SEQ ID NO:5), T_{12} (SEQ ID NO:6), A_{12} (SEQ ID NO:7), G_{12} (SEQ ID NO:8), and their interactions with their complementary strands).

Example 11

Scaffold-Specific Single Molecule Raman Signals

[0178] For Au and Ag nanoclusters, as one moved to excitation wavelengths longer than the characteristic plasmon absorptions (~390 nm for Ag, ~520 nm for Au), transition strengths became extremely strong due to collective oscillation of electrons. The plasmon in such nanoscale metal species is more discrete in nature and leads to the unprecedented strong emission. As shown in Figures 17 and 18, these species were readily observable on the single molecule level with excitation strengths up to 100 times stronger than the best organic dyes. It is precisely these extremely strong optical

transitions that can lead to very high polarizabilities and to single molecule Raman (SM-Raman) signals from the scaffold or encapsulating material encapsulating the sub-nm noble metal nanocluster. Thus, the SM-Raman can be used advantageously for *in vivo* biolabeling.

[0179] By exciting slightly longer wavelength than both the optical transition and the surface plasmon excitation, strong, blinking, SM-Raman spectra were observed from the Ag and Au dendrimer and peptide encapsulated individual nanodots (Figs. 17A-F). The peptide-encapsulated nanodots had strong SM-Raman signals with narrow features characteristic of the peptide scaffold. With Ag nanoclusters as the contrast agents, these highly scaffold specific Raman signals were readily observed under 514-nm excitation (Figs. 17D-F), while Au nanodots may need to be excited in the near IR to yield SM-Raman transitions, both in accord with SM-SERS signals observed from dyes adsorbed on surfaces of much larger Ag and Au nanoparticles. These observations demonstrated that only the nanocluster (not the large nanoparticle) interacting with the organic scaffold was necessary to produce Raman signals on the single molecule level and yield the observed wavelength dependence on excitation. Consequently, SM-Raman did not need large nanoparticles to be observed on the single molecule level – the few-atom-sized, strongly absorbing, pre-plasmonic Ag or Au nanoclusters were sufficient to yield strong SM-Raman signals with 100x larger cross-sections than the best organic fluorophores and emission rates >100x higher than even much larger semiconductor quantum dots due to the extremely fast and efficient radiative decay (Peyser-Capadona *et al.*, Phys. Rev. Lett. 2005, 94: 058301).

[0180] While individual molecules had very different spectra, each was specific to the surrounding scaffold. Additionally, by only looking within a very narrow spectral window corresponding to the vibrational frequency shift from the laser energy, the strong, very narrow (vibrational) linewidth further reduced background but maintained very strong single molecule signals. Whether individual features were probed with Raman spectroscopy or the spectra of many individual features were summed (Fig. 18A-C), clear differences were observed that are characteristic of the nanodot-encapsulating scaffold. By exciting longer than the surface plasmon frequency of the bulk metal, the enhanced Raman was clearly observed on the single molecule level. It is this observation that allows for the use SM-Raman as an *in vivo* label with chemical information. Because of the narrow linewidths, an order of magnitude increase in sensitivity was possible solely due to background reduction of

the broad autofluorescence by looking in a narrow spectral window that contains only the Raman emission.

[0181] The noble metal nanodots were very stable in both solution (even at high salt concentrations) and films and were readily observed on the single molecule level with chemically tunable emission properties, ultrabright fluorescent and scaffold-specific SM-Raman emission and reduced blinking (Fig. 19).

Example 12

SM-Raman signals arise from the Scaffold

[0182] The experiments in Example 12 were performed using the Ag nanoclusters produced with both PAMAM G4-OH and G2-OH dendrimers (fourth- and second-generation OH-terminated poly(amidoamine)) and SEQ ID NO:1 discussed in Example 11.

[0183] The Raman transitions were so strong that even the Anti-stokes (AS) lines were readily observed on the single molecule level (Fig. 20A,C). At $1/80^{th}$ of the strength of the 1550 cm^{-1} Stokes shifted line, these higher energy transitions were stronger than expected from a thermal distribution of scaffold excited vibrational state populations. As high-intensity conditions for potential optical pumping were not present in this work (Kneipp *et al.*, J. Am. Chem. Soc. 2004, 76:2444), the observed deviation from a thermal distribution and quadratic dependence on excitation intensity may have resulted from preferential AS enhancement due to a recently reported metal-molecule charge transfer (Brolo *et al.*, Phys. Rev. 2004, 69:045424). Exhibiting identical shifts to the Stokes-shifted transitions, these higher energy AS-Raman features also blinked (Fig. 20B) and occurred on top of a weak background of currently unknown origin. AS spectra were excited at the same $30W/cm^2$ intensities at 514.5 nm and were collected at 10 second exposures through short pass optics to image the higher energy emission. Stokes and AS emission from the exact same encapsulated nanoclusters were measured by switching filters within the microscope filter turret during the same data set. This was the first observation of single molecule AS-Raman and provides true background free windows for biological imaging by measuring emission at higher energy than the excitation (Cheng *et al.*, Biophys. J. 2002, 83: 502). With the AS signal being ~$1/80^{th}$ of the Stokes lines, AS-Raman transitions exhibited intensities comparable to standard single molecule fluorescence from the best organic

dyes. As observed with the Stokes-shifted lines, the SM-Anti-stokes of the peptide (not shown) and of the PAMAM were distinctly different and the frequencies of each match their respective Stokes-shifted counterparts. All Raman lines and fluorescent backgrounds were also observed when excited closer to resonance at 476 nm.

[0184] The observed total absorption cross sections were comparable to those observed for Ag nanoclusters on roughened thin Ag and AgO films as well as those encapsulated in PAMAM dendrimers in solution ($\sigma = 10^{-14}$ cm^2) (Peyser *et al.*, Science 2001, 291: 103; Zheng & Dickson, J. Am. Chem. Soc. 2002, 124: 13982). Accordingly, both the SM-Raman and Ag_n fluorescence likely stemmed from initial Ag nanocluster electronic excitation. While not being limited to this interpretation, since the laser excitation is well overlapped with the electronic absorption of the silver nanoclusters (Bonacic-Koutecky *et al.*, J. Chem. Phys 2001, 115: 10450), a type of resonance or pre-resonance enhancement likely occurs, but without plasmon enhancement as our few-atom Ag nanoclusters are too small to support such a collective electron oscillation. As metal nanoclusters are highly polarizable (Ho *et al.*, J. Chem. Phys. 1990, 93: 6987; Hild *et al.*, Phys. Rev A 1998, 57: 2786; Spasov *et al.*, J. Chem Phys Lett. 1999, 110: 5208) and exhibit giant resonances in their gas phase photofragmentation (Tiggesbaumker *et al.*, Chem. Phys. Lett 1992, 190: 42) and photoelectron-ejection spectra (Henglein *et al* Faraday Discuss 1991, 92:31), it is possible that either a predissociative or photoelectron ejection process is accessed in the excited state leading to significant transfer of charge to the scaffold and significant Franck-Condon overlap with the scaffold vibrational levels. While the scaffold stabilizes the Ag nanocluster and prevents photodissociation characteristic of gas phase Ag_n (Ho *et al.*, J. Chem. Phys. 1990, 93: 6987; Hild *et al.*, Phys. Rev A 1998, 57: 2786; Spasov *et al.*, J. Chem Phys Lett. 1999, 110: 5208; Tiggesbaumker *et al.*, Chem. Phys. Lett 1992, 190: 42), a large excited state charge separation most likely produces the large oscillator strength, fast radiative lifetime, and Raman-enhancing ability of these few-atom nanoclusters. Consequently, the Raman transitions seem to "piggy-back" off the strong Ag nanocluster optical transition to yield the strong SM-Raman signals.

Example 13

Chemical Derivatization of the Scaffold Provides a Unique Single Molecule Raman Signal

[0185] Functional groups as Raman labels are incorporated into the dendrimer core. A variety of functional groups including carbon-deuterium (C-D) and triple bonds (C≡N, C≡C, C≡O) have vibrational frequencies outside the fingerprint and hydrogen stretching regions in the nearly background-free 1900~2300 cm^{-1} spectral region. Using the proper excitation wavelength and especially using time-gated detection, SM-Raman offers nearly background–free imaging even in biological media.

[0186] Deuterium labeled dendritic cores are used initially, along with carbon-carbon triple bonds. Figure 21 outlines the proposed dendrimer cores.

[0187] Cores 1 and 2 contain deuterium instead of hydrogen on key carbons and are based on the original PAMAM core. Both cores are either commercially available (Core 1) or can be synthesized using standard PAMAM creation conditions: exhaustive Michael addition of amino groups with methyl acrylate followed by amidation of the resulting ester with ethylenediamine (Core 2) (Esfand & Tomalia, Drug Discov. Today 2001, 6: 427-436; Grayson & Frechet, Chem Rev. 2001, 101: 3819-3867; Hecht *et al.,* J. Polym. Sci. Part A: Polym. Chem. 2003, 41:1047-1058). This strategy allows the placement of a deuterium label in any dendrimer generation by using ethylene-d_4-diamine instead of ethylenediamine. A library of PAMAM dendrimers of generation 1-5 are synthesized *via* the divergent dendrimer synthesis approach with deuterium labels in each generation. This library allows the study and determination of the optimal location and concentration of the Raman label in the dendrimer through single molecule Raman and fluorescence microscopy.

[0188] Cores 3-6 contain one or more carbon-carbon triple bond. These compounds are either commercially available (Core 3) or can be synthesized in one or two steps using standard palladium coupling chemistry (Cores 4-6). These cores are designed to a) increase systematically the amount (and ultimately the concentration) of the carbon-carbon triple bonds in the core to determine the optimal C≡C triple bond concentration and b) to study the effect of the number of dendrons (for example, Core 3 has one acetylene unit and two alcohols which allow for two dendron-functionalization. In contrast, Core 4 has also only one acetylene unit but four alcohols) on the proposed application. These cores may be used for either convergent (pre-synthesized dendrons assembled with the core molecule in the last step) or divergent (starting from the dendrimer core and building the dendrimer outwards) PAMAM syntheses (Grayson & Frechet, Chem Rev. 2001, 101: 3819-3867).

Dendron and basic dendrimer design and synthesis.

[0189] PAMAM dendrimers are synthesized easily *via* convergent or divergent methodologies and with amine, alcohol, ester, or acid functionalities on the surface. In particular the convergent approach allows for the synthesis of multifunctionalized dendrimers using different dendrons. The most common PAMAM synthesis follows the divergent synthetic strategy outlined above in the core section by exhaustive Michael addition of amino groups with methyl acrylate followed by amidation of the resulting ester with ethylenediamine and extensive HPLC purification (Esfand & Tomalia, Drug Discov. Today 2001, 6: 427-436; Grayson & Frechet, Chem Rev. 2001, 101: 3819-3867; Hecht *et al.*, J. Polym. Sci. Part A: Polym. Chem. 2003, 41:1047-1058). Using Cores 1 and 2, this approach is used to synthesize dendrimers of generations 1-5. Due to the nature of the divergent methodology, these dendrimers will contain only amine functionalities on the surface, *i.e.* they are monofunctionalized, and will be functionalized as outlined in Figure 22, strategy C (Dendrimers 1). Furthermore, using literature procedures, a variety of dendrons are synthesized based on the Michael-addition/amidation approach (Dendrons 1) for use in the convergent dendrimer methodology. Based on a recent report by Newkome and coworkers, bifunctionalized dendrons are synthesized using the 1→2+1 C-branching monomer (MFCBU 1) (Newkome *et al.*, Macromol. 2003, 122: 6139-6144). Newkome demonstrated the synthesis of monofunctionalized second-generation PAMAM-analog dendrons with a single second functional group on the surface, *i.e.* all but one functional groups on the surface were either esters or acids resulting in a bifunctionalized dendrimer with a single second functionality on the surface. The lone surface alcohol group allows for subsequent specific mono-functional attachment of a single moiety onto the dendrimer surface. Using complementary chemistry and MFCBU 1 dendrons of generation 1-5 are synthesized with well-defined multifunctional surfaces (Dendrons 2). The non-MFCBU 1 containing complementary generations 1-5 dendrons are also synthesized, *i.e.* dendrons with a purely acid or ester containing surface (Dendrons 3). Furthermore, in analogy to the methodology described by Newkome, MFCBU 2 containing two alcohol groups and a single ester or acid group are designed and synthesized using standard chemistry. Using protection and deprotection steps, generation 1-5 dendrons with variable concentrations of MFCBU 2 are synthesized (Dendrons 4) resulting in dendrons with mainly alcohol

functionalities and one or more (based on the design and synthesis) acid functionality. Furthermore, the non-MFCBU 2, *i.e.* non-acid containing dendron-analogs to Dendrons 4 are synthesized yielding Dendrons 5. These five different dendrons provide a) a toolbox of dendrons with different surface functionalities and different degrees of surface multifunctionalization and b) the opportunity to design and synthesize dendrimers with well-defined functional groups, thereby allowing a modular approach toward dendrimer synthesis.

[0190] The composite dendrimers with Raman tags and pre-programmed surface functionalities are synthesized using standard chemistry by reacting the dendrons with the dendrimer cores outlined above. In some cases an alkyl spacer with a terminal acid functionality is introduced onto the core molecules thereby changing the functional group from an alcohol to an acid allowing for standardized amide formations between the cores and the terminal amines of the first generation of the dendrons. As outlined above, the proposed core molecules provide the opportunity to vary the number of dendrons per dendrimer from two to six and ultimately control the extent of multifunctionalization on the surface of the desired and designed dendrimer. Again, through variations of the different dendrons used, the design and synthesize dendrimers that are mostly amine, alcohol, or acid functionalized, each containing a controlled number (one or more) of acid or alcohol functionalities is allowed. Furthermore, through dendron variations, dendrimers are synthesized with a mixture of alcohols and acids each functionality class located on a single side of the globular dendrimer. For example, a 50% alcohol and 50% acid dendrimer could be a two-dendron dendrimer based on one dendron from Dendron 5 and one from Dendron 3 or a 33% alcohol and 67% acid dendrimer would be based on a three-dendron dendrimer based on one dendron from Dendron 5 and two from Dendrons 3. In summary, this modular dendron/core convergent synthesis approach allows for the controlled multifunctionalization of dendrimer surfaces while simultaneously incorporating Raman tags as acetylene or C-D bonds at controlled locations throughout the core and branches.

Incorporation of modularity in biospecificity: Dendrimer surface functionalization

[0191] To incorporate biospecific recognition units and Raman labels and/or peptide sequences for peptide mediated protein delivery into cells, orthogonal multifunctionalization schemes are developed. To minimize different surface chemistries, a modular surface functionalization scheme is desirable. The requirements

for such a functionalization scheme are that the chemical transformations are fast and quantitative, can be carried out under mild reaction conditions, can be generalized to a wide variety of potential functional groups, and are orthogonal to each other. In most cases, PAMAM dendrimers have been functionalized using amide or ester formations or through thiourea linkages. Unfortunately, these transformations are not orthogonal to each other. 1,3-dipolar cyclo-additions or 'click' chemistry is therefore used as the second orthogonal transformation to multifunctionalize dendrimer surfaces (Wang *et al.*, J. Amer. Chem. Soc. 2003, 125: 3192-3193; Katritzy & Singh, J. Org. Chem. 2002, 67: 9077-9079; Speers *et al.*, J. Amer. Chem. Soc. 2003, 125: 4686-4687; Jeong & O'Brien *et al.*, J. Org. Chem. 2001, 66: 4799-4802). 'Click' chemistry between an azide and an acteylene unit is known to proceed quantitatively in water under very mild reaction conditions, and is tolerant to a wide variety of functional groups including amines, acids, and alcohols (*Id.*). The only functional groups intolerant with 'click' chemistry are triple bonds and phosphines. The dendrimers are designed to not contain any phosphines or triple bonds on the surface of the dendrimers. The acteylene units in the core of the dendrimers are inaccessible to functionalized dendrimer surfaces due to the globular shape of the dendrimers and steric repulsions. Therefore, 'click' chemistry is orthogonal to all functionalization on the dendrimer surface and is the second chemical transformation of choice.

[0192] Azides are one of the two essential parts of 'click' chemistry and are stable to functional groups and most reaction conditions. Azides, therefore, are one preferred functional group for the 'click' chemistry on the dendrimer surface. As described above, dendrimers are created with a wide variety and controllable density of surface functional groups. The terminal alcohol moieties of the dendrimer surface are designed to be the 'click' chemistry anchoring unit. Transformation of the alcohols into azides will be carried out in a three-step synthetic sequence. The resulting dendrimers will have either protected amine or acid functionalities and a well-defined number of azide groups on the surface. After deprotection, the dendrimers may be bifunctionalized in an orthogonal fashion by using 'click' chemistry to attach one functional group onto the dendrimer and using standard ester or amide formation protocols or thiourea linkages for the second functionalization giving us the unique possibility to bifunctionalize dendrimers for biological applications in a predesigned and well-controlled manner. This methodology could also allow for triple surface functionalization by first using 'click' chemistry followed by a difunctionalization of

the remaining surface functionalities using the stoichiometric difunctionalization strategy outlined in Figure 22B.

[0193] Dendrimers are synthesized using a) ethylene-*d4*-diamine as the core followed by standard divergent dendrimer synthesis to yield the final amine functionalized dendrimer and b) Core 4 which is functionalized with four dendrons (three dendrons containing only surface acid functionalities and one dendron based on MFCBU 1) using the convergent dendrimer approach to give a bifunctionalized dendrimer that contains only one terminal alcohol moiety. These two dendrimers allow the study of the monofunctionalization strategy as well as acetylenes and C-D Raman labels. Further dendrimers are generated containing all proposed cores and dendrons.

SM-Raman studies

[0194] Because the Raman enhancement is a local effect, controlled Raman tag placement within the dendrimer identifies the position of the nanocluster within each dendrimer based on the specific vibrational transitions it enhances. By studying the Raman signal of C-D bonds (~2050 cm^{-1}) placed in different shells according to the synthetic procedure above, the position of the nanocluster within the dendrimer core and how to further improve the optical signal is understood. Optimization of the Raman signals will allow more vibrational modes to be incorporated, thereby creating even stronger emissive labels.

[0195] As Raman is an instantaneous inelastic scattering process, it has an extremely fast lifetime component (<100 fs) and is therefore very strong and narrow compared with fluorescence. Using time correlated single photon counting (tcspc) to determine relative contributions from fluorescence and Raman at each wavelength, the optimal excitation wavelengths for each color of Ag and Au nanoclusters is determined to optimize the unique Raman signals. Furthermore, lifetime measurements down to 10 ps both in bulk and on single nanodots are possible and routinely performed. The extremely fast lifetime provides yet another important sensitivity enhancement opportunity. By gating the detection to only collect the strongly emitting fast component, complete discrimination against typical nsec lifetime background fluorescence is capable in order to isolate the nanocluster fast fluorescence (Ag) and Raman components, or for Au, just the instantaneous Raman component. This time discrimination will greatly enhance the sensitivity of *in vivo* single molecule imaging with these unique nanodots. Together with the previously measured fluorescence

quantum yields, the excitation wavelengths are optimized to preferentially produce the Raman and fluorescence signals of interest.

Example 14

Multiphoton and non-linear excitation of encapsulated nanoclusters

[0196] Harmonic generation microscopy, of which two examples are second harmonic and third harmonic microscopy resulting from doubling and tripling the incident laser frequency (energy), respectively, was performed using these noble metal nanoclusters as indicated by the observed spectra in Figure 23. In this experiment, second generation PAMAM-encapsulated Ag nanoclusters were excited with 860-nm light from a pulsed ~200 fs, 84 MHz titanium:sapphire laser. The emitted spectrum showed emission at higher energy than used to excite the individual nanocluster with broad strong two-photon excited emission (fluorescence, continuum generation, and Raman) and a narrow peak at twice the excitation energy, or half the wavelength, ~430 nm, corresponding to second harmonic generation. Darkfield microscopy confirmed that this strong emission and harmonic generation resulted from individual encapsulated, sub-31 metal atom noble metal nanoclusters, without large nanoparticles being present or necessary to see emission. The doubled light suggests application as contrast agents in multiphoton or harmonic generation microscopy and potentially in general second harmonic generation applications.

[0197] The strong two-photon-excited emission (higher energy than the exciting 860-nm laser and lower energy than the second harmonic peak at 430-nm) exhibited a shorter excited state lifetime than that resulting from single photon excitation at 430-nm. This broad emission was excited with a two-photon cross section of greater than 10^5 GM and was actually comparable to or larger than any two-photon excited emission observed from any other single entity. These will find great application as multiphoton excited fluorescent labels. The short lifetime produces extremely high count rates and the very strong two-photon (or in general multiphoton) cross section indicates that very low intensity pulsed excitation may be utilized for excitation, thereby making these very useful two-photon excited emissive dyes, whether measuring the doubled light or the fluorescence/emission upon multiphoton excitation. Overall these emissions shown in Figure 24 exhibit a non-linear, and nearly quadratic dependence on the incident intensity, thereby indicating that they arise from a two-photon process. The second harmonic generation and need for pulsed laser

excitation to observe the fluorescence indicate that this is a simultaneous multiphoton excitation, with a instrument response limited lifetime of less than 7-picoseconds as indicated by the indistinguishability of the 35-ps instrument response and the measured nanocluster emission decay (Fig. 25).

5